Endosomal pH in neuronal signaling and synaptic transmission: Role of Na+/H+ exchanger NHE5

Article *in* Frontiers in Physiology · January 2014

DOI: 10.3389/fphys.2013.00412 · Source: PubMed

2 authors:

Graham H Diering
Johns Hopkins Medicine
16 PUBLICATIONS **285** CITATIONS
SEE PROFILE

Masayuki Numata
University of British Columbia - Vancouver
51 PUBLICATIONS **1,536** CITATIONS
SEE PROFILE

Endosomal acidification by Na^+/H^+ exchanger NHE5 regulates TrkA cell-surface targeting and NGF-induced PI3K signaling

Graham H. Diering[a,*,†], Yuka Numata[a,*], Steven Fan[a], John Church[b], and Masayuki Numata[a]
[a]Department of Biochemistry and Molecular Biology and [b]Department of Cellular and Physiological Sciences, University of British Columbia, Vancouver, BC V6T 1Z3, Canada

ABSTRACT To facilitate polarized vesicular trafficking and signal transduction, neuronal endosomes have evolved sophisticated mechanisms for pH homeostasis. NHE5 is a member of the Na^+/H^+ exchanger family and is abundantly expressed in neurons and associates with recycling endosomes. Here we show that NHE5 potently acidifies recycling endosomes in PC12 cells. NHE5 depletion by plasmid-based short hairpin RNA significantly reduces cell surface abundance of TrkA, an effect similar to that observed after treatment with the V-ATPase inhibitor bafilomycin. A series of cell-surface biotinylation experiments suggests that anterograde trafficking of TrkA from recycling endosomes to plasma membrane is the likeliest target affected by NHE5 depletion. NHE5 knockdown reduces phosphorylation of Akt and Erk1/2 and impairs neurite outgrowth in response to nerve growth factor (NGF) treatment. Of interest, although both phosphoinositide 3-kinase–Akt and Erk signaling are activated by NGF-TrkA, NGF-induced Akt-phosphorylation appears to be more sensitively affected by perturbed endosomal pH. Furthermore, NHE5 depletion in rat cortical neurons in primary culture also inhibits neurite formation. These results collectively suggest that endosomal pH modulates trafficking of Trk-family receptor tyrosine kinases, neurotrophin signaling, and possibly neuronal differentiation.

Monitoring Editor
Patrick J. Brennwald
University of North Carolina

Received: Jun 20, 2012
Revised: Aug 21, 2013
Accepted: Aug 28, 2013

INTRODUCTION

One of the principal characteristics of neuronal differentiation is the induction of membrane protrusions that develop into neurites, which in turn become discernible as axons and dendrites as the neuron becomes polarized (Arimura and Kaibuchi, 2007). Vesicular trafficking serves as a major mechanism for supplying membrane components to rapidly growing neurite tips and delivers surface receptors, including the Trk family of receptor tyrosine kinases that mediate the effects of neurotrophins on neuronal development and survival (Bradke and Dotti, 1998; Ledesma and Dotti, 2003; Sann *et al.*, 2009; Meldolesi, 2011). Trk receptors synthesized at the soma are targeted to the neurite tips by anterograde transport and initiate neurotrophin (ligand)-dependent downstream signaling, which triggers neurite outgrowth (Huang and Reichardt, 2001; Chao, 2003). On ligand binding, Trk receptors are internalized to a series of endosomes via retrograde transport; some populations of receptors are targeted to lysosomes for degradation, whereas others are recycled back to the cell surface. The importance of vesicular trafficking in Trk signaling is further reinforced by the finding that receptor-mediated signaling can occur in endosomes after receptor internalization (Baass *et al.*, 1995; Murphy *et al.*, 2009; Sorkin and von Zastrow, 2009). Thus, elucidating the molecular mechanisms underlying Trk receptor targeting is of crucial importance for understanding neurotrophin-mediated signaling.

The acidic luminal pH milieus of organelles along both anterograde and retrograde trafficking pathways are tightly regulated, and progressive acidification along these pathways is required for correct sorting and routing of endosomal cargoes (Mellman *et al.*, 1986;

This article was published online ahead of print in MBoC in Press (http://www.molbiolcell.org/cgi/doi/10.1091/mbc.E12-06-0445) on September 4, 2013.

*These authors contributed equally.

†Present address: Department of Neuroscience and Howard Hughes Medical Institute, Johns Hopkins University School of Medicine, Baltimore, MD 21205.

Address correspondence to: Masayuki Numata (mnumata@mail.ubc.ca).

Abbreviations used: Arf6, ADP-ribosylation factor 6; ARNO, ARF nucleotide-binding site opener; BCECF, 2′-7′-bis(carboxyethyl)-5(6)-carboxyfluorescein; EEA1, early endosome antigen 1; FBS, fetal bovine serum; GFP, green fluorescent protein; HA, hemagglutinin; HBS, HEPES-buffered saline; NGF, neuron growth factor; NHE, sodium-hydrogen exchanger; NKA, Na^+/K^+-ATPase; PBS, phosphate-buffered saline; PI3K, phosphoinositide 3-kinase; RFP, red fluorescent protein; shRNA, short hairpin RNA; SNX17, sorting nexin-17; Tfn, transferrin; TfnR, transferrin receptor; Trk, tropomyosin-receptor-kinase; V-ATPase, vacuolar-type H^+-ATPase.

Supplemental Material can be found at:
http://www.molbiolcell.org/content/suppl/2013/09/02/mbc.E12-06-0445.DC1.html

Presley *et al.*, 1997; Bacac *et al.*, 2011). Although it is generally accepted that the vacuolar-type H^+-ATPase proton pump (V-ATPase) plays a pivotal role in organellar acidification by pumping protons into lumens (Forgac, 2007; Marshansky and Futai, 2008), establishment of the distinct pH environments in different endosomal fractions cannot be explained solely by V-ATPase activity, and the participation of other proton-translocating mechanisms such as organellar ion transporters and channels is essential to establish and maintain the distinct organellar pH milieus (Casey *et al.*, 2010; Scott and Gruenberg, 2011). Neurons contain a more sophisticated endosomal system, which permits neuron-specific targeting and signaling (Winckler and Mellman, 2010; Li and Difiglia, 2012). Given the importance of endosomal pH in vesicular trafficking, it is likely that a diverse array of proton transport mechanisms govern endosomal pH homeostasis in neurons. Of particular interest in this regard is NHE5, a unique member of the Na^+/H^+ exchanger family abundantly expressed in neuron-rich regions of brain (Attaphitaya *et al.*, 1999; Baird *et al.*, 1999). We showed previously that *N*-methyl-D-aspartate receptor activation leads to recruitment of NHE5 to the cell surface at the synapse, where it regulates activity-dependent local pH changes and dendritic spine growth (Diering *et al.*, 2011). At steady state, NHE5 is largely associated with endosomes (Lukashova *et al.*, 2013), predominantly recycling endosomes (Szaszi *et al.*, 2002). However, the functional significance of NHE5 in the recycling endosome, a key organelle that regulates multiple vesicular trafficking pathways (Maxfield and McGraw, 2004; Grant and Donaldson, 2009; Hsu and Prekeris, 2010; Huotari and Helenius, 2011; Urbanska *et al.*, 2011), is an open question. Rat pheochromocytoma PC12 cells express the TrkA receptor tyrosine kinase and extend neurites upon nerve growth factor (NGF) stimulation, serving as an excellent model in which to study neurotrophin-mediated signal transduction pathways and vesicular trafficking (Greene and Tischler, 1976; Vaudry *et al.*, 2002; Martin and Grishanin, 2003; Habauzit *et al.*, 2011; Harrill and Mundy, 2011). Here we show that NHE5 potently acidifies recycling endosomal pH, regulates TrkA receptor cell-surface abundance, and promotes neurite outgrowth in PC12 cells treated with NGF.

RESULTS

NHE5 is functional in recycling endosomes

We previously reported that NHE1 and NHE5 are the two major NHEs expressed in PC12 cells and generated short hairpin RNA (shRNA) PC12 cell lines that have constitutively reduced expression of these proteins (Diering *et al.*, 2011). Using cell-surface biotinylation and Western blot, we observed that little NHE5 is present on the plasma membrane, whereas NHE1 and transferrin receptor (TfnR) are abundantly expressed on the plasma membrane of resting PC12 cells (Figure 1A). Actin was not detectable on the cell surface, indicating that membrane integrity was retained during these experiments. To test for NHE5 activity on the cell surface, we loaded PC12 cells with the pH-sensitive fluorescent dye 2′-7′-bis(carboxyethyl)-5(6)-carboxyfluorescein (BCECF) and monitored the recovery of cytosolic pH (pH_i) from an imposed intracellular acid load using the ammonium prepulse technique (Figure 1B). After washout of ammonium with Na^+-free buffer, pH_i failed to recover from the internal acid load and remained acidic until the reintroduction of external Na^+, at which time it rapidly recovered to normal values. The specific NHE1 inhibitor cariporide (10 μM; Masereel *et al.*, 2003) completely prevented the recovery of pH_i observed after the reintroduction of external Na^+ and, in agreement with previous work (Szabo *et al.*, 2000), 10 μM cariporide failed to inhibit NHE5 activity heterologously expressed in NHE-deficient Chinese hamster ovary mutant AP-1 cells (Supplemental Figure S1). These findings indicate that NHE1, but not NHE5, is the major functional NHE on the plasma membrane in PC12 cells.

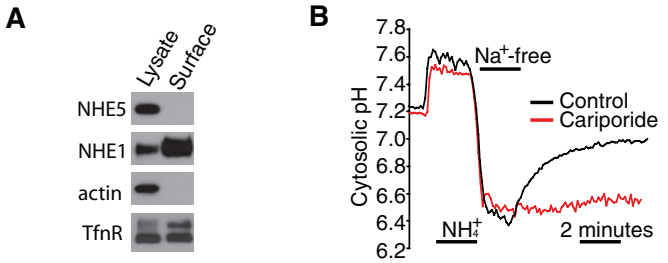

FIGURE 1: NHE5 is not functional on the plasma membrane in resting PC12 cells. (A) PC12 cells were treated with a cell-surface biotinylating agent. Biotinylated cell-surface proteins were purified by affinity trap with NeutrAvidin beads. Total lysate (Lysate) and biotinylated proteins eluted from the beads (Surface) were resolved in SDS–PAGE and immunoblotted with the indicated antibodies. Lysate protein fractions represent 10% of the protein loaded in the surface fraction. (B) Cells loaded with BCECF were subjected to cytosolic acidification by briefly exposing cells to NH_4Cl followed by washout with NaCl-free solution. NHE activity was induced by reintroducing the Na^+-containing solution in the absence or presence of the NHE1-specific inhibitor cariporide (10 μM). No recovery from the internal acid load was observed in the presence of cariporide, indicating that NHE1 is the only functional NHE on the plasma membrane in PC12 cells. Records represent pH_i measurements obtained simultaneously from 40 control and 34 cariporide-treated cells and are representative of three independent experiments under each condition.

Previous studies showed that NHE5 is largely associated with recycling endosomes under steady-state conditions (Szaszi *et al.*, 2002, Szabo *et al.*, 2005; Diering *et al.*, 2009). We next tested the possible involvement of NHE5 in recycling endosomal pH regulation. Control PC12 cells or PC12 cells stably expressing NHE5-shRNAs (described in Diering *et al.*, 2011) were incubated with a mixture of two types of transferrin (Tfn), one conjugated with the pH-sensitive fluorescent dye fluorescein and the other conjugated with the pH-insensitive dye Alexa Fluor 568, to generate a ratiometric reporter of recycling endosomal pH. Cells were rinsed three times with prewarmed serum-free media and transferred to the preheated (37°C) stage of a confocal microscope, and 15 min later, image capture began for fluorescein/Alexa Fluor 568 emission intensity ratio measurements. Under these conditions, Tfn was observed mainly in perinuclear structures (Figure 2B), a distribution typical of recycling endosomes (Figure 2C). The fluorescence ratios collected from live-cell imaging were calibrated to endosomal pH using the high–$[K^+]$/nigericin technique (Presley *et al.*, 1997; D'Souza *et al.*, 1998; Sonawane *et al.*, 2002; Brett *et al.*, 2005; Ohgaki *et al.*, 2010). In control PC12 cells, recycling endosomal pH was 6.20 ± 0.02 (SEM), whereas in shNHE5 cells recycling endosomal pH was 6.48 ± 0.02, a value significantly more alkaline than in parental PC12 cells (Figure 2A). After 5-min treatment with the V-ATPase inhibitor bafilomycin, we observed endosomal alkalinization to pH 6.52 ± 0.02 in control PC12 cells and 6.75 ± 0.03 in shNHE5 cells (Figure 2A). These results suggest that NHE5 is a potent recycling endosomal acidifier, playing an equally important role as the V-ATPase in PC12 cells. We next addressed the effect of NHE5 knockdown on early endosomal pH using a previously described protocol with some modifications (Gagescu *et al.*, 2000). As shown in Supplemental Figure S2, there was no significant difference in early endosomal pH between the two cell lines (pH = 6.06 ± 0.02 in PC12 cells vs. 6.01 ± 0.02 in shNHE5 cells).

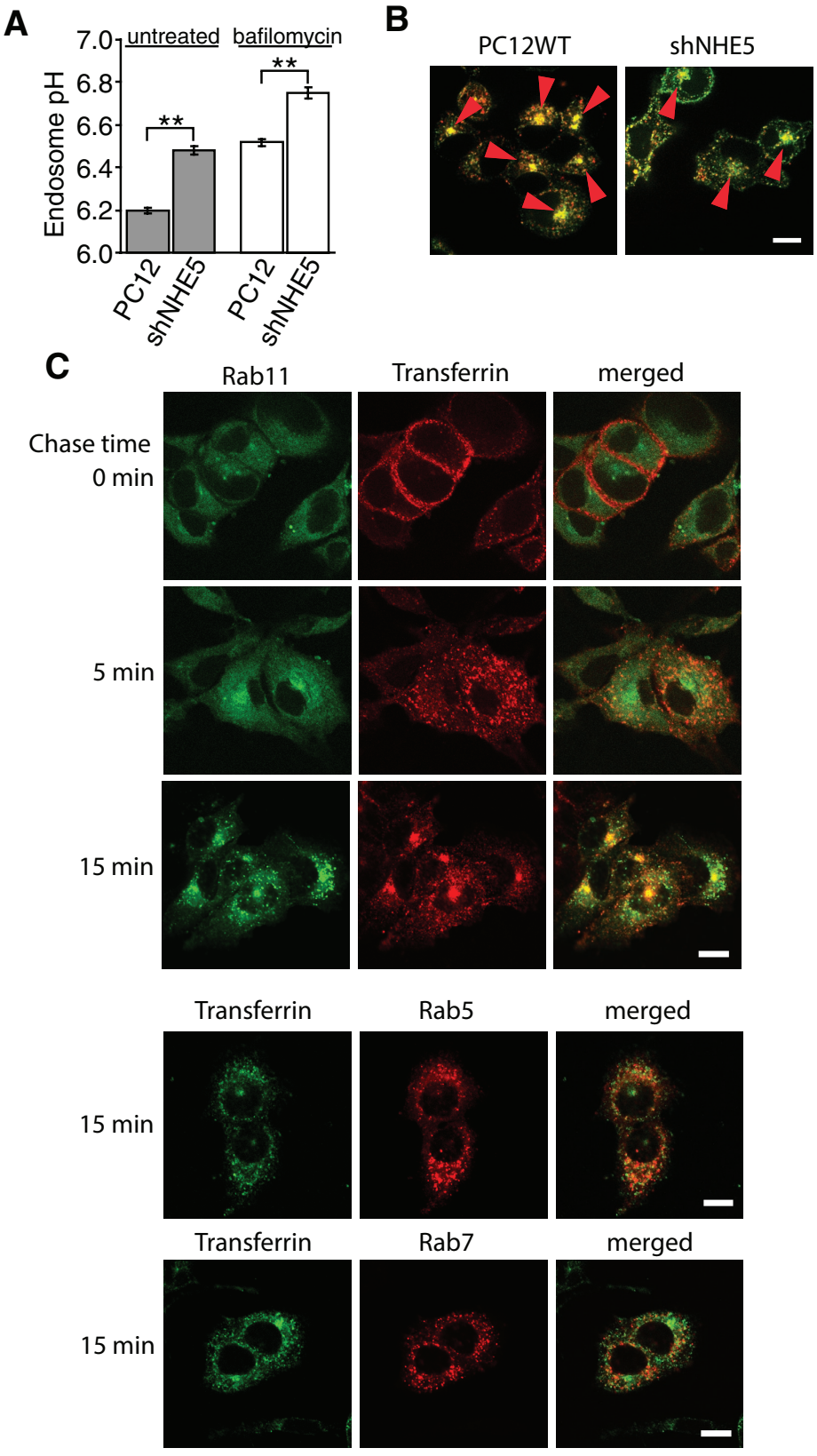

FIGURE 2: NHE5 is potent acidifier of recycling endosomes. (A) Endosomal pH in control PC12 cells and shNHE5 cells in the presence or absence of bafilomycin treatment. A mixture of fluorescein-conjugated (pH-sensitive) and Alexa Fluor 568–conjugated (pH-insensitive) transferrin was used as a ratiometric recycling endosomal pH reporter. $N = 100–200$ cells per condition. Error bars represent SEM, $^{**}p < 0.01$ (Student's t test). (B) A set of representative live-cell images used for pH measurement experiments. Fluorescence signals for transferrin associated with perinuclear structures (arrowheads) were captured under live-cell confocal imaging and analyzed for pH determination (see *Materials and Methods*). Scale bar, 10 μm. (C) Double immunofluorescence labeling of transferrin and endosomal markers. PC12 cells were treated with Alexa Fluor 568–conjugated transferrin and subjected to chase incubation under the same condition as in A and B. Rab11 antibody, heterologously expressed mCherry-tagged Rab5, and mCherry-tagged Rab7 were used to visualize recycling and early and late endosomes, respectively. Scale bars, 10 μm.

NHE5 participates in TrkA trafficking

NGF-induced differentiation in PC12 cells involves NGF signaling through the high-affinity receptor tyrosine kinase TrkA and the low-affinity p75 receptor (Huang and Reichardt, 2001; Vaudry *et al.*, 2002; Chao, 2003). TrkA traffics between the cell surface and the recycling endosomal compartment, and this recycling controls the steady-state surface abundance and activity of TrkA (Arimura *et al.*, 2009; Ascano *et al.*, 2009; Vaegter *et al.*, 2011). Consistent with this, we found that TrkA exhibits some association with the recycling endosomal marker Rab11 at the perinuclear region and, to a lesser extent, the early endosomal marker EEA1 (Figure 3A, PC12). Reduced NHE5 expression did not disrupt the endosomal association of TrkA (Figure 3A, shNHE5). Because NHE5 is predominantly associated with endosomal compartments in hippocampal neurons in primary culture (Diering *et al.*, 2011), we addressed whether NHE5 and TrkA associate in endosomes of PC12 cells. NHE5 and TrkA exhibited close association mostly in intracellular compartments (Figure 3B). To test the potential involvement of NHE5 in TrkA trafficking behavior, we next examined the total and cell-surface abundance of TrkA by surface biotinylation and Western blot. There was no difference in the total abundance of TrkA between control cells and PC12 cells stably expressing shNHE5 or shNHE1 (Figure 4, A and C), suggesting that reduced expression of NHE5 or NHE1 has little effect on TrkA degradation or synthesis. In contrast, the cell-surface abundance of TrkA was significantly reduced in cells expressing shRNA for NHE5 (shNHE5; by approximately half) compared with control PC12 cells or PC12 cells expressing shRNA for NHE1 (shNHE1; Figure 4, A and D). When cell lysates were not incubated with the biotinylating agent, TrkA was not detected (Figure 4B). Similar levels of

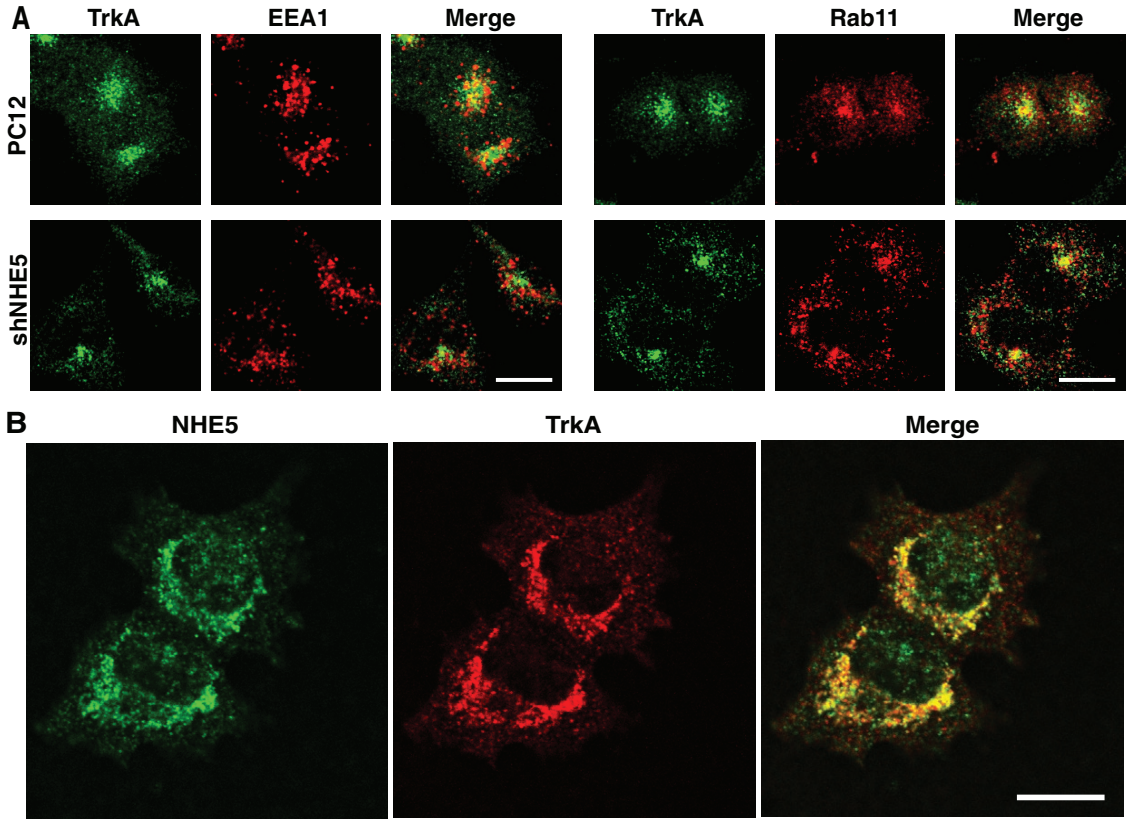

FIGURE 3: Intracellular localization of TrkA and NHE5. (A) Double immunofluorescence microscopy of TrkA (green) and EEA1 (red) or Rab11 (red) in PC12 control cells (PC12) and PC12 cells stably expressing shRNA for NHE5 (shNHE5). Fixed cells were treated with rabbit polyclonal anti-TrkA antibody and mouse monoclonal anti-EEA1 antibody or anti-Rab11 antibody. Alexa Fluor 488–conjugated goat anti-mouse and Alexa Fluor 568–conjugated goat anti-rabbit antibodies were used to visualize the signals. (B) Double immunofluorescence microscopy of NHE5 (green) and TrkA (red) in PC12 cells. Fixed cells were treated with rabbit polyclonal anti-NHE5 antibody and mouse monoclonal anti-TrkA antibody to visualize the endogenous protein localization. Scale bars, 10 μm.

cell-surface populations of Na^+/K^+ ATPase pump α-subunit and TfnR across the cell lines were observed (Figure 4, A and E), suggesting the specific effects of NHE5 on TrkA trafficking. After NGF treatment, there was a time-dependent reduction in cell-surface TrkA abundance in control PC12 cells (Figure 4, F and G), as reported previously (Grimes *et al*., 1996; Jullien *et al*., 2002; Kuruvilla *et al*., 2004; Chen *et al*., 2005). To test the potential involvement of NHE5 in NGF-induced TrkA internalization, shRNA-expressing cells were treated with NGF for the indicated times, and TrkA retained on the cell surface was detected by biotinylation (see *Materials and Methods*). Although the initial cell-surface abundance of TrkA is significantly lower in shNHE5 cells than in shNHE1 or control cells (time 0, Figure 4F), densitometric analysis showed that the rates of NGF-induced TrkA endocytosis were comparable among the three cell lines (Figure 4G). These results suggest that knockdown of NHE5 but not NHE1 reduces steady-state TrkA abundance on the cell surface but not overall TrkA protein levels or rates of endocytosis. To test whether TrkA trafficking from recycling endosomes to the plasma membrane is affected by NHE5 knockdown, we next determined recycling rates of biotinylated TrkA from endosomes to the plasma membrane. As shown in Figure 4, H and I, a slight but significant delay in recycling rates was detected in shNHE5 cells.

Organelle alkalinization redistributes TrkA

Our data are consistent with the possibility that NHE5 may be a novel regulator of recycling endosomal pH to influence the trafficking of TrkA between endosomes and the plasma membrane. To further test this hypothesis, we examined the effect of bafilomycin on TrkA cell-surface abundance. Treatment of control PC12 cells with bafilomycin (250 nM) caused a significant decrease in TrkA surface abundance after 5–6 h of bafilomycin treatment but not in total TrkA protein expression (Figure 5, A and B). The cell-surface abundance of TfnR, another recycling receptor, was not noticeably affected by bafilomycin. Bafilomycin treatment, which is known to lead to organellar alkalinization, resulted in the accumulation of TrkA inside the cell similar to that observed in cells with stable knockdown of NHE5. Taken together, these results suggest that steady-state trafficking of TrkA through recycling endosomes is sensitive to endosomal pH.

NHE5 knockdown affects NGF signaling

Because NHE5 knockdown affects TrkA trafficking and its cellular distribution, we reasoned that NHE5 might modulate TrkA downstream signaling. Control PC12 or shNHE5 cells were treated with 50 ng/ml NGF for 0–60 min, and the phosphorylation status of Akt (also known as PKB) and ERK1/2, two major downstream kinases, were evaluated by Western blot using antibodies that specifically recognize phosphorylated Akt and Erk1/2, respectively. NGF treatment of serum-starved PC12 cells caused a clear increase in the phosphorylation levels of Akt and Erk1/2 within 5 min. In contrast, phosphorylated Akt in response to NGF was significantly suppressed in shNHE5 cells under the same experimental conditions (Figure 6,

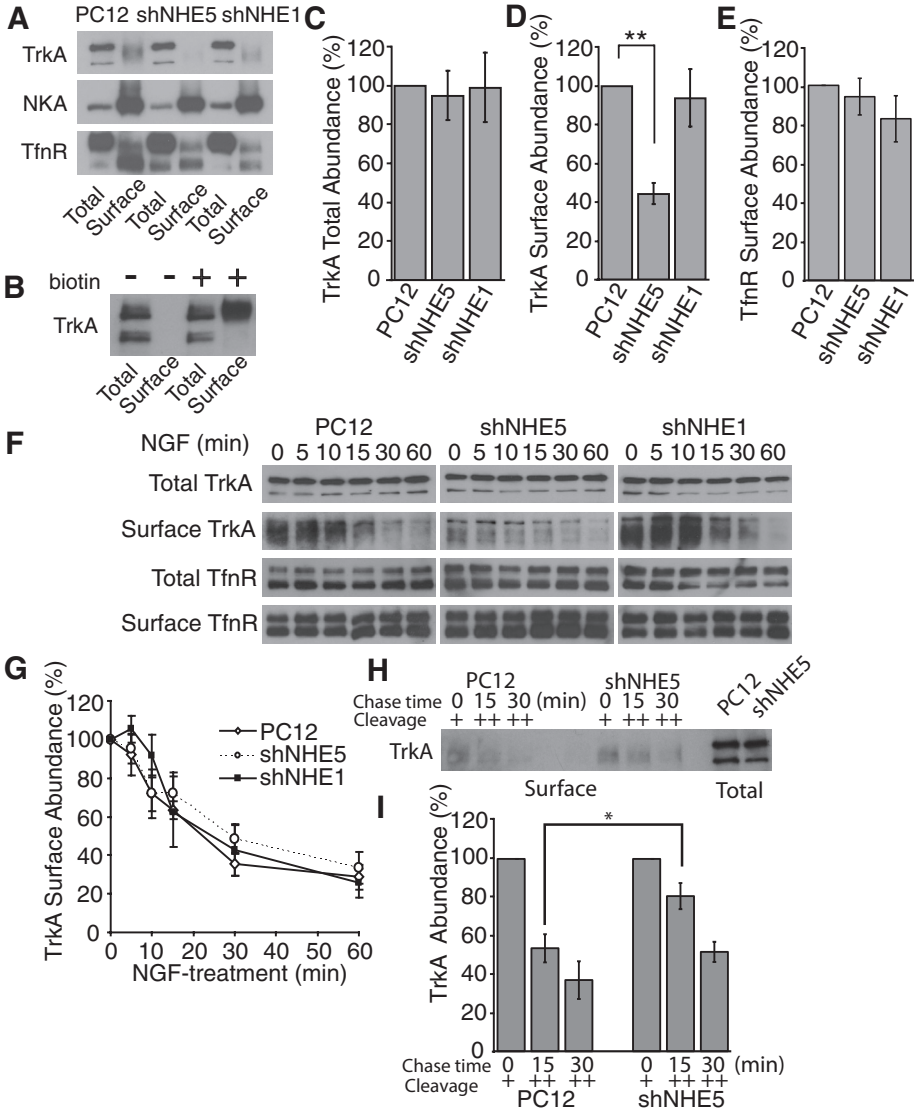

FIGURE 4: NHE5 knockdown affects TrkA steady-state surface abundance but not NGF-induced internalization. (A–E) Control PC12 cells (PC12) and PC12 cells stably expressing shRNAs against NHE5 (shNHE5) or NHE1 (shNHE1) were incubated with a cell-surface biotinylation reagent, and total and cell-surface TrkA, NKA, or TfnR were detected by Western blot. Western blot shown in A is representative of three independent experiments. (B) No-biotin control confirmed that there was no fraction being pulled down nonspecifically. The intensity of the bands was determined by densitometry, and the data represent the mean ± SEM of relative levels of total TrkA (C), cell-surface TrkA (D), and TfnR (E) of at least three experiments. $^{**}p < 0.01$ (paired Student's *t* test compared with control). (F, G) Cells were serum starved overnight and then treated with 50 ng/ml NGF as indicated, and the total and cell-surface abundance of TrkA, as well as of TfnR, at each time point were determined. Western blots shown are representative of three independent experiments. (G) Relative NGF-induced TrkA endocytosis was measured by quantifying the TrkA cell-surface abundance at various times after NGF treatment. The rate of TrkA endocytosis was not different between the cell lines tested. Error bars represent SEM. (H, I) After surface biotinylation, cells were incubated for 60 min at 37°C. Biotin remaining on cell-surface proteins was removed by glutathione, and then cells were subjected to the second incubation with NGF (50 ng/ml) at 37°C for 0, 15, or 30 min and treated with glutathione to remove biotin from the proteins recycled back to the plasma membrane, and relative TrkA abundance was determined. For pull down, 130 and 400 µg of total protein were used for PC12 and shNHE5 cells, respectively. The densitometry data of relative levels of total TrkA are presented with mean ± SEM. $^{*}p < 0.05$ (paired Student's *t* test, $n = 6$ experiments).

point (Figure 6, B and D). Of interest, although shNHE1 cells showed weaker and delayed Akt phosphorylation in response to NGF treatment, Erk1/2 phosphorylation was not affected. To examine the role of endosomal alkalinization in NGF-TrkA signaling, we treated PC12 cells with bafilomycin for 6 h, a condition that significantly reduced cell-surface TrkA levels (Figure 5, A and B), and assessed its effect on NGF-induced phosphorylation of Akt and Erk1/2. Bafilomycin treatment markedly decreased NGF-induced phosphorylation of Akt (~20% of control) and Erk1/2 to a lesser extent (~60% of control; Figure 7, A–C). Thus NHE5 knockdown and bafilomycin treatment commonly have a greater effect on the phosphorylation of Akt than the phosphorylation of Erk1/2 in response to NGF stimulation. Of interest, 1-h bafilomycin treatment, a condition that did not affect TrkA cell-surface abundance, reduced Akt phosphorylation but not Erk1/2 phosphorylation (Figure 7, D–F).

NHE5 and neurite outgrowth

Having shown that NHE5, a significant endosomal acidifier in PC12 cells, influences the cell-surface abundance of TrkA and the downstream signaling of NGF-TrkA, we postulated that NHE5 might modulate NGF-induced neurite outgrowth. Control PC12 cells and PC12 cells expressing shNHE5 or shNHE1 were treated with NGF (50 ng/ml) for 72 h, followed by fixation and cytochemical visualization of actin and tubulin as a reliable read-out of cellular morphology. After NGF treatment, cells were examined for the presence or absence of neurite extensions of at least 15 µm in length emanating from the cell body (Sin *et al.*, 2009). Compared to control cells, in which nearly 50% of the cells extended neurites, only ~20% of shNHE5 cells formed neurites (Figure 8, A and C). Moreover, the shNHE5 cells that did form neurites exhibited a significant reduction in total neurite number and length compared with the control cells (Figure 8, B, D, and E). This reduction in neurite outgrowth was seen in multiple shNHE5 clones using three independent shRNA constructs (Supplemental Figure S3). Of interest, shNHE1 cells showed a small but significant increase in the number of cells forming neurites (Figure 8, A and C), a trend opposite to that observed in shNHE5 cells. However, in shNHE1 cells that did form neurites, the mean total neurite number and length were significantly reduced (Figure 8, A–D), in agreement with our previous study showing that pharmacological inhibition or genetic ablation of NHE1 adversely affect neurite elongation and branching (Sin *et al.*, 2009). Thus, whereas knockdown of either NHE5 or NHE1 led to reductions

A and C). Erk1/2 phosphorylation in shNHE5 cells was reduced at the 5-min time point, reaching ~30% of that observed in control cells, and then formed a slightly delayed peak at the 10-min time

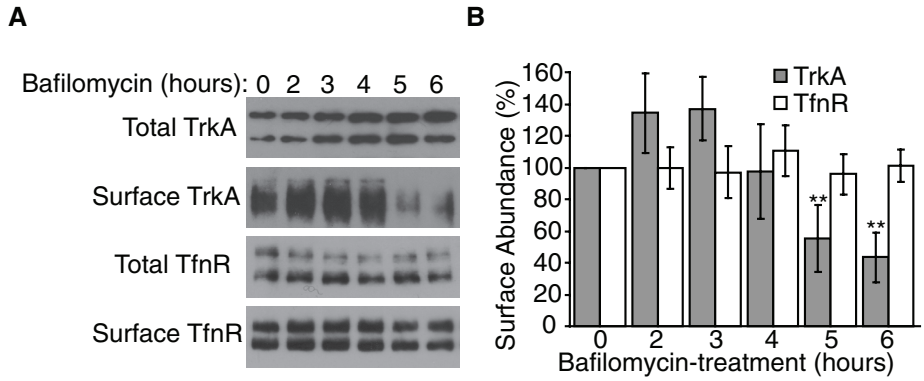

FIGURE 5: Bafilomycin treatment reduces TrkA surface levels. (A) Serum-starved PC12 cells were incubated with bafilomycin A1 (250 nM) for the times indicated, and cell-surface TrkA or TfnR was detected by surface biotinylation assay. (B) TrkA or TfnR cell-surface abundance was determined by densitometry, and relative intensities were calculated. $N = 3$; error bars represent SEM; $^{**}p < 0.01$ (Student's t test) for difference from untreated cells (time 0).

in neurite number and length in cells that actually formed neurites, only knockdown of NHE5 impaired the cell's ability to differentiate in response to NGF treatment, as evidenced by the reduced number of cells with any neurite formation (Figure 8C). To further investigate the specificity of the effects of shRNA, we generated double stable cells expressing both shNHE5 and hemagglutinin (HA)-tagged human NHE5 ($NHE5_{36HA}$), which has a sequence different from that of rat NHE5 and is resistant to shNHE5 (Diering *et al.*, 2011). The defective neurite morphology observed in shNHE5 cells was partially rescued in the double stable cells (Figure 9, A–D). We next tested whether heterologously expressed NHE5 can rescue the defective NGF-induced signaling observed in shNHE5 cells. As shown in Figure 9, E–G, NHE5 expression significantly increased phosphorylation of Akt and Erk1/2 in response to NGF stimulation. Finally, we transiently transfected shNHE5 into rat cortical neurons in primary culture and examined the effect on neurite formation. As shown in Figure 10, A–C, both neurite number and length were slightly but significantly reduced as a result of shNHE5 expression. Although TrkA may be expressed in cultured cortical neurons, depending on culture conditions (Counts *et al.*, 2004), TrkB is the predominant Trk receptor in cortex (Barbacid, 1994; Huang and Reichardt, 2001). Thus it will be important to test the effect of NHE5 on TrkB trafficking behavior and signaling.

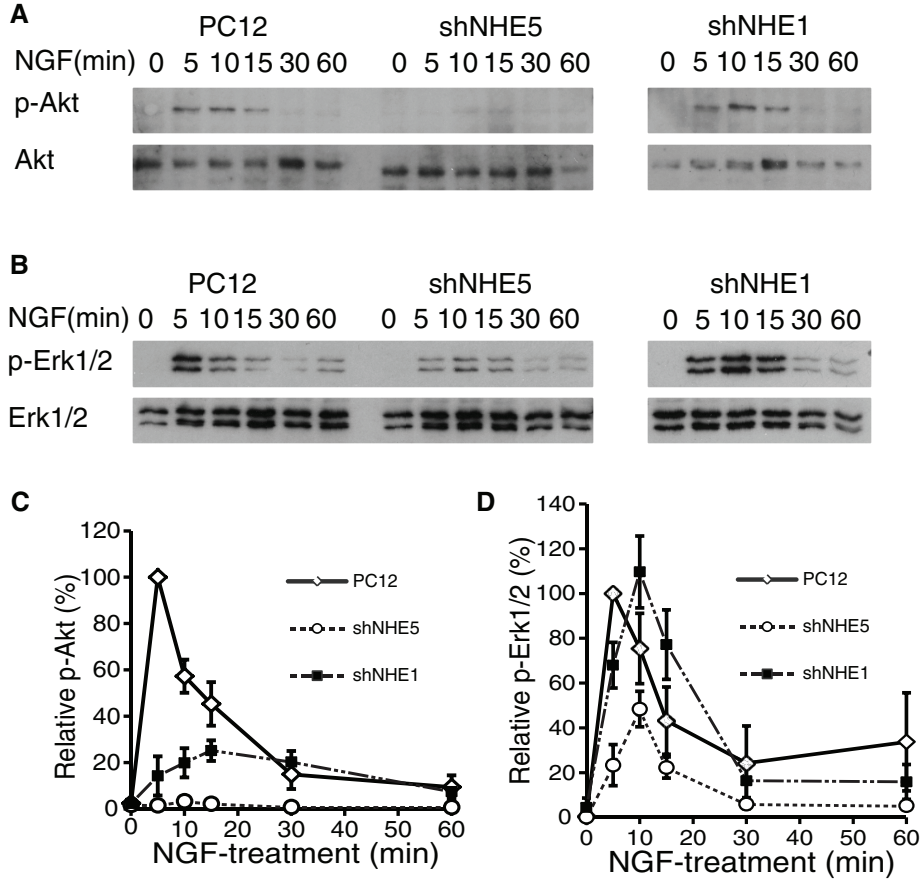

FIGURE 6: NHE5 knockdown affects NGF signaling. (A–D) Control PC12, shNHE5, and shNHE1 cells were serum starved overnight and then treated with 50 ng/ml NGF for the indicated times. The amounts of phosphorylated and total Akt and Erk1/2 were detected by Western blot (A and B, respectively). Representative Western blots are shown. The experiments were repeated three times, and the intensities of the bands were determined by densitometry. The relative levels of phospho-Akt (C) and phospho-Erk1/2 (D) are expressed as means ± SEM.

DISCUSSION

Endosomes are functionally and morphologically heterogeneous organelles, and certain types of cells, such as neurons and epithelial cells, possess more complex endosomal systems than those in fibroblasts (Weisz and Rodriguez-Boulan, 2009; Golachowska *et al.*, 2010; Winckler and Mellman, 2010; Huotari and Helenius, 2011). In addition, recycling endosomal pH varies among different types of cells. For example, Madin–Darby canine kidney cells, a widely used model for polarized epithelial cells, have more acidic recycling endosomal compartments than those in Chinese hamster ovary cells (Gagescu *et al.*, 2000; Wang *et al.*, 2000), although the underlying mechanisms remain to be elucidated. In the present study, we identified the neuron-enriched ion transporter NHE5 as an endosomal pH regulator and showed that NHE5 knockdown diminishes cell-surface targeting of TrkA and impairs NGF signaling and neurite extension. Recycling endosomal pH in PC12 cells (pH = ~6.20) is found to be more acidic than the previously reported value in Chinese hamster ovary cells (pH ≈ 6.5), which do not express NHE5 (Presley *et al.*, 1997). Recycling endosomal pH in PC12 cells stably expressing shRNA for NHE5 (shNHE5 cells; pH ≈ 6.48) was close to the value observed in Chinese hamster ovary cells, and treatment of shNHE5 cells with a V-ATPase inhibitor further alkalinized recycling endosomes. Moreover, preliminary findings suggest that NHE-deficient

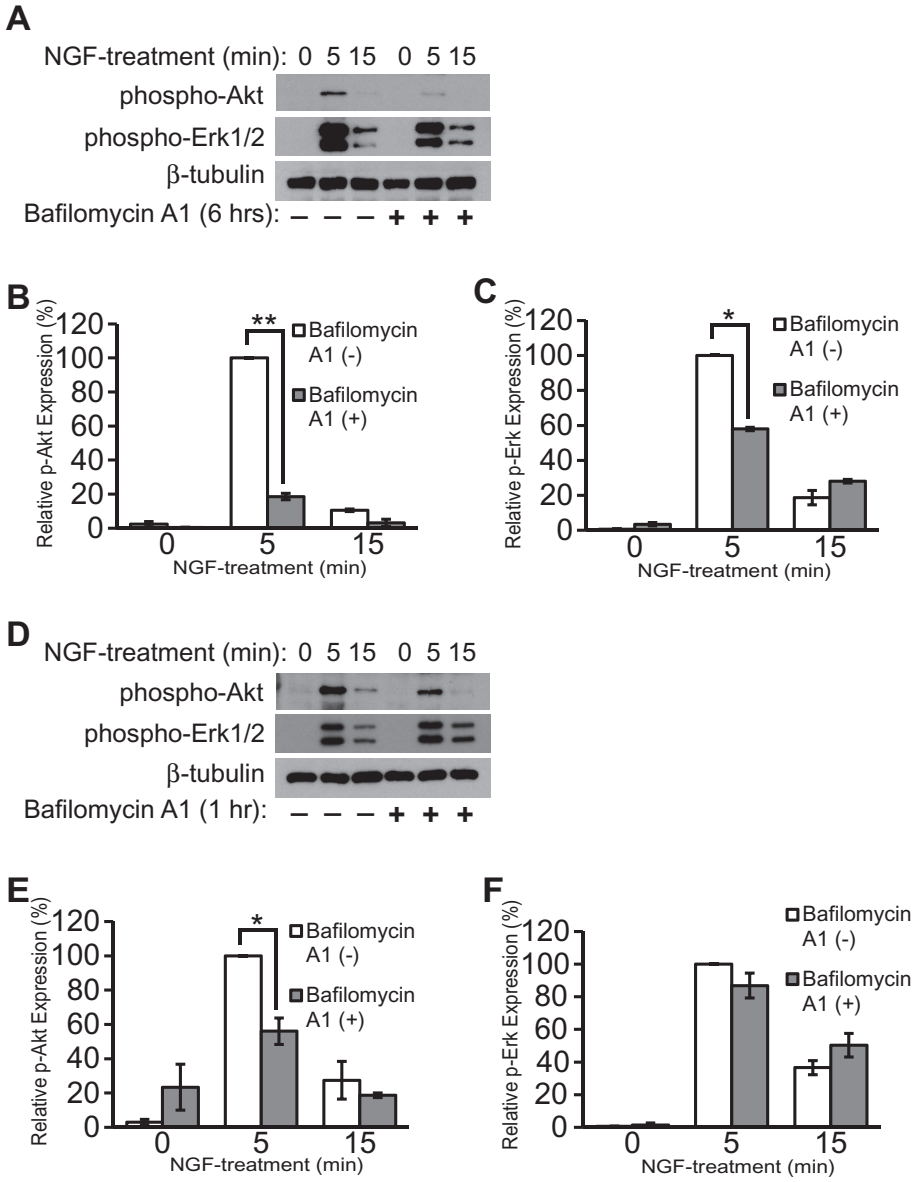

FIGURE 7: Bafilomycin A1 treatment affects NGF-TrkA signaling. Serum-starved PC12 cells were incubated in the absence (–) or presence (+) of 250 nM bafilomycin A1 for 6 h (A) or 1 h (D), and cells were stimulated with NGF (50 ng/ml) for the indicated periods. Whole-cell lysates (5 µg of protein) were subjected to SDS–PAGE and probed with anti–phospho-Akt, anti–phospho-Erk1/2, and anti–β-tubulin antibodies. Levels of phospho-Akt (B, E) and phospho-Erk1/2 (C, F) were quantified by densitometry and expressed as relative values to these observed at 5 min of NGF treatment in bafilomycin A1–untreated cells. Representative Western blots are shown in A and D. Densitometric data summarize three independent experiments and are presented as mean ± SEM. *$p < 0.05$, **$p < 0.01$ (paired Student's *t* test).

Chinese hamster ovary mutant AP-1 cells have a recycling endosomal pH of 6.63 ± 0.05 ($N = 263$, mean ± SEM), close to the value (pH = 6.73) previously reported by D'Souza *et al.* (1998). Intriguingly, AP-1 cells stably expressing human NHE5 exhibited recycling endosomal pH of 6.33 ± 0.03 ($N = 268$, mean ± SEM), close to that observed in PC12 cells (Y.N. and G.H.D., unpublished data). Although we have to be cautious about the interpretation of these data (in light of the nonphysiological nature of the AP-1 cell experimental system, ambient expression levels of heterologously expressed NHE5, and its potential mislocalization), these findings obtained under the same conditions using the pH-sensitive fluorescent transferrin probe support the possibility that NHE5 and V-ATPase are the two separate physiological mechanisms that acidify recycling endosomes. NHE5 is responsible for endosomal acidification of PC12 cells and contributes to the establishment of a more acidic endosomal pH in PC12 than in Chinese hamster ovary cells. To our knowledge, this is the first molecule identified as a PC12 cell–specific endosomal acidifier. Treatment with the V-ATPase inhibitor bafilomycin also diminished the cell-surface targeting of TrkA and suppressed NGF-induced TrkA signaling in PC12 cells. Furthermore, Ascano *et al.* (2009) showed that the protonophoric drug monensin leads to the intracellular accumulation of TrkA, a phenotype similar to that observed after depletion of NHE5 or bafilomycin treatment. These results collectively suggest that endosomal pH homeostasis by NHE5 plays a key role in the proper targeting of TrkA. Endosomal lumens are originally continuous with the extracellular space when vesicles are formed on the plasma membrane. In this regard, it is interesting that extracellular acidification has been suggested to increase the cell-surface targeting of TrkA (Bray *et al.*, 2013).

We showed that perturbation of endosomal pH by NHE5 knockdown affects the cell-surface targeting of TrkA but not that of the Na^+/K^+-ATPase α-subunit (NKA). Our finding that depletion of NHE5 does not influence the internalization rate of TrkA is consistent with a previous study indicating that perturbation of endosomal pH does not affect retrograde NGF signaling or NGF-TrkA binding affinity in endosomes (Harrington *et al.*, 2011). Moreover, reversible biotinylation experiments suggested that the rate of TrkA targeting from recycling endosomes to the plasma membrane is impaired in NHE5-knockdown cells. These results indicate that impaired anterograde trafficking of TrkA via the recycling pathway primarily accounts for diminished signaling and defective neurite formation in NHE5-knockdown PC12 cells. A remarkable diversity of receptor recycling has been reported, and some integral membrane proteins follow recycling pathways distinct from that of transferrin receptors, a well-recognized marker for the bulk recycling pathway. Recent studies have started to reveal some mechanisms for cargo-specific recycling. For example, ligand-induced recycling of β2-adrenergic receptors, but not δ-opioid receptors, is facilitated by actin-stabilized endosomal tubules (Puthenveedu *et al.*, 2010). More recently, an unbiased screening identified β integrins as cargoes whose recycling is facilitated by the FERM-like domain–containing sorting nexin SNX17 (Steinberg *et al.*, 2012). We propose that endosomal pH is a novel regulatory factor for cargo-specific non–bulk recycling pathways. Previous studies showed that bafilomycin treatment markedly decreases the exit rate of TfnR from recycling endosomes to the plasma

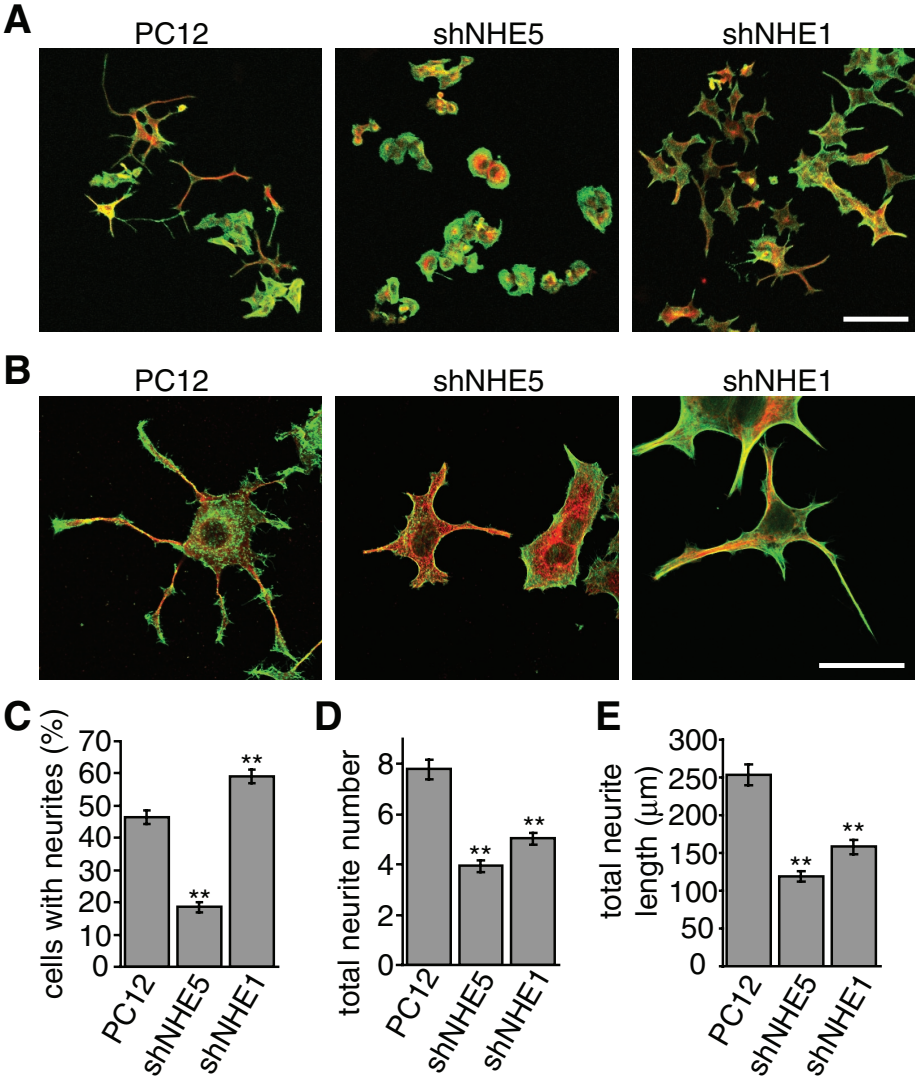

FIGURE 8: NHE5 modulates NGF-induced neurite growth in PC12 cells. (A, B) Control PC12 cells or PC12 cells stably expressing NHE5 shRNA (shNHE5) or NHE1 shRNA (shNHE1) were treated with 50 ng/ml NGF for 72 h to induce differentiation. Cells were labeled to visualize actin (green) and tubulin (red). Scale bars, 100 μm (A), 40 μm (B). (C) The percentage of cells in the population that formed at least one neurite ≥15 μm in length. In all cases $N = 1700–1800$ cells; error bars represent SEM; $^{**}p < 0.01$ (Student's t test) for difference from control cells. (D, E) Mean total neurite number (D) and length (E) in individual cells that had clearly differentiated (at least one neurite ≥15 μm in length). Under each condition $N \geq 80$ cells.

membrane in Chinese hamster ovary cells (Presley *et al.*, 1997). However, we were not able to discern any effect of bafilomycin, nor were we able to see reproducible effects of NHE5 knockdown on cell-surface targeting of TfnR in PC12 cells. It has been reported that iron homeostasis is greatly influenced when yeast (Diab and Kane, 2013) and mammalian cells (Straud *et al.*, 2010) are treated with bafilomycin. In addition, TfnR expression in some mammalian cell lines is up-regulated by treatment with bafilomycin (Straud *et al.*, 2010). Thus we cannot completely rule out the possibility that endosomal pH affects TfnR trafficking in PC12 cells, an effect that might have been masked by unknown compensatory mechanisms under our experimental conditions. An alternative possibility is that cell type–specific targeting mechanisms contribute to TfnR targeting (Clague *et al.*, 1994; van Weert *et al.*, 1995), and endosomal pH–dependent targeting may occur in a cell type–dependent manner. Careful follow-up studies are needed to resolve these issues.

Reduced cell-surface abundance of TrkA as a result of NHE5 depletion or pharmacological inhibition of V-ATPase should diminish NGF-induced phosphorylation of Akt and Erk to a similar extent. In fact, the maximum phosphorylation levels of Erk were reduced and the time after NGF treatment required to reach the maximum phosphorylation level was delayed as a consequence of NHE5 knockdown or V-ATPase inhibition. Unexpectedly, however, NGF-induced phosphorylation of Akt was more severely impaired than Erk phosphorylation. Most intriguingly, 1-h bafilomycin treatment, the condition that did not noticeably affect TrkA cell-surface abundance or Erk-phosphorylation, significantly decreased NGF-induced Akt phosphorylation. These results raise the interesting possibility that endosomal pH influences Akt phosphorylation in addition to TrkA trafficking. Phosphoinositide 3-kinase (PI3K)–Akt signaling occurs in endosomes in various cell types (Garcia-Regalado *et al.*, 2008; Schenck *et al.*, 2008; Tsutsumi *et al.*, 2009; Walz *et al.*, 2010; Fujioka *et al.*, 2011; Nazarewicz *et al.*, 2011), including NGF-treated PC12 cells (Lin *et al.*, 2006; Varsano *et al.*, 2006), and endosomal Akt signaling contributes to persistent NGF-TrkA signaling after the ligand–receptor complex is endocytosed (Harrington *et al.*, 2011). Recruitment of not only class II and class III PI3Ks, whose association with endosomes is well recognized, but also class I PI3K to endosomes and their possible activation therein has been suggested (Vanhaesebroeck *et al.*, 2010). Genetic studies in *Drosophila* and *Caenorhabditis elegans* suggest the possible involvement of receptor tyrosine kinases in class II PI3K signaling. Although much less is known about the role of receptor tyrosine kinases in class III PI3K signaling, there is evidence that class III PI3Ks are regulated by G protein–coupled receptors (Slessareva *et al.*, 2006), indicating that class III PI3Ks may be activated by extracellular stimuli. Mounting evidence points to the possibility that endosomal membranes provide a location for signaling (Miaczynska *et al.*, 2004; Murphy *et al.*, 2009; Sadowski *et al.*, 2009; Scita and Di Fiore, 2010; Platta and Stenmark, 2011). The small endosomal lumen may define a discrete microenvironment segregated from the cytosol and regulate protein–protein and/or protein–lipid interactions required for signaling. It is interesting to speculate that endosomal pH might coordinate PI3K-Akt signaling by modulating the protonation and charge status of the signaling components. Early endosomes, including the Rab5-positive compartment and EEA1-positive fraction, are well documented as a potential location where intrinsic signaling arises (Garcia-Regalado *et al.*, 2008; Sigismund *et al.*, 2008; Sorkin and von Zastrow, 2009). Recent studies reveal the involvement of late endosomes/lysosomes in endosomal signaling (Flinn *et al.*, 2010; Sancak *et al.*, 2010; Taelman *et al.*, 2010; Zoncu *et al.*, 2011; Dobrowolski *et al.*, 2012; Jewell

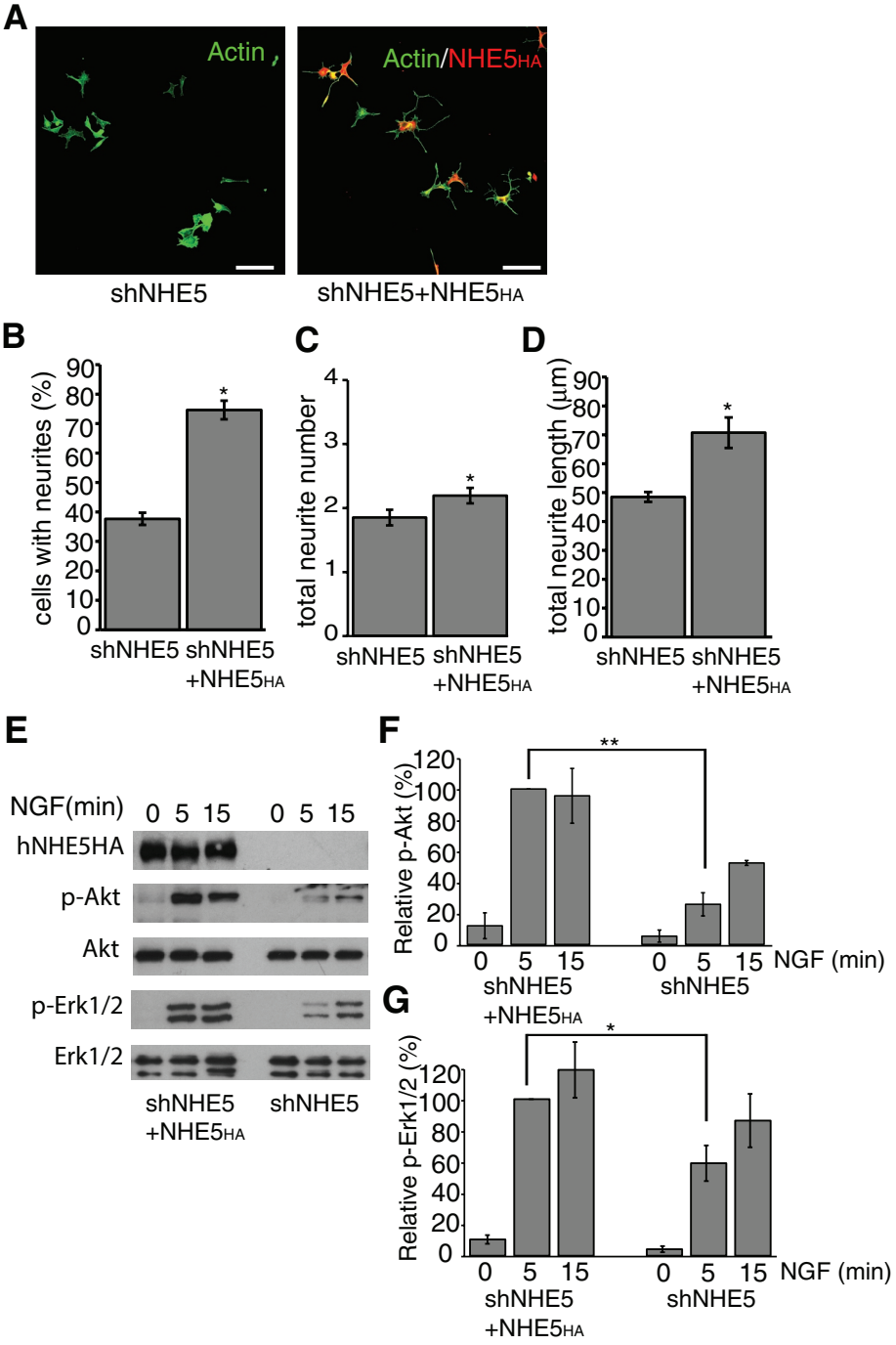

FIGURE 9: Stable expression of $NHE5_{36HA}$ reverses phenotypes of NHE5-deficient PC12 cells. (A) NGF-induced neurite outgrowth phenotype of shNHE5 cells stably expressing control vector or shRNA-resistant, HA-tagged human NHE5 ($NHE5_{36HA}$). Anti-HA antibody (red) and fluorescently labeled phalloidin (green) were used to visualize F-actin and NHE5, respectively. Scale bar, 50 μm. The percentage of cells with at least one neurite extension (B), mean total neurite number (C), and length (D) in individual cells that had clearly differentiated (at least one neurite ≥15 μm in length). $N \geq 150$ cells in each cell type per experiment; error bars represent SEM of $n = 3$ experiments; $^*p < 0.05$ (paired Student's t test) for difference from control cells. (E, F) shNHE5 cells stably expressing control vector or shRNA-resistant, HA-tagged human NHE5 ($NHE5_{36HA}$) were serum starved overnight and then treated with 50 ng/ml NGF for the indicated times. The amounts of phosphorylated and total Akt and Erk1/2 were detected by Western blot. (E) Representative Western blots. The experiments were repeated three times, and the intensities of the bands were determined by densitometry. The relative levels of phospho-Akt (F) and phospho-Erk1/2 (G) are expressed as means ± SEM.

et al., 2013). We propose a model in which signal is generated and amplified in endocytic recycling compartments in a pH-dependent manner.

A prolonged incubation with bafilomycin for 5–6 h was needed to achieve an equivalent effect on TrkA targeting as NHE5 knockdown, implicating the possible involvement of additional factor(s). A recent genome-wide screening of a shRNA library identified V-ATPase subunits as essential molecules for clathrin formation during endocytosis (Kozik *et al.*, 2013). Intriguingly, however, prolonged bafilomycin treatment for up to 24 h was needed to elicit a similar effect on clathrin formation. The authors hypothesized that the constant delivery of membrane components (e.g., cholesterol) by endocytic recycling is required for clathrin formation and that the proper acidic endosomal pH is required for mobilizing membrane components. Similarly, membrane lipids or proteins supplied from other organelles in the endocytic recycling loop may be gradually depleted upon V-ATPase inhibition, and this in turn may slow down anterograde trafficking of TrkA. It is also of note that the action of NHE5 is more restricted to recycling endosomes, whereas inhibition of V-ATPases should have a broader effect on virtually all acidic organelles. If spatially restricted neutralization of recycling endosomes is important, V-ATPase inhibition may not elicit as strong an effect as NHE5 knockdown. To address these possibilities and uncover the underlying mechanism(s), it will be important to deplete V-ATPase subunit genes and examine their effects on TrkA trafficking.

An NHE1 gene defect is responsible for slow-wave epilepsy in mutant mice (Cox *et al.*, 1997). We previously showed that NHE1 is targeted to growth cones and alkalinizes the cytosol during NGF-induced differentiation of PC12 cells (Sin *et al.*, 2009). More recent work showed that NHE1 is associated with axonal termini and growth cones and suggested that NHE1 regulates axonal survival of Purkinje cells (Liu *et al.*, 2013). NHE1 and NHE5 appear to regulate neuronal differentiation via different mechanisms. First, in contrast to the proposed axonal function of NHE1 (Liu *et al.*, 2013), a recent immunohistochemical study suggested that NHE5 is predominantly localized to somatodendritic areas (Lukashova *et al.*, 2013). Although we cannot exclude the possible involvement of NHE5 in axonal functions, NHE1 and NHE5 may be targeted to distinct neuronal domains and play different roles, a situation analogous to basolaterally associated NHE1 and apically targeted

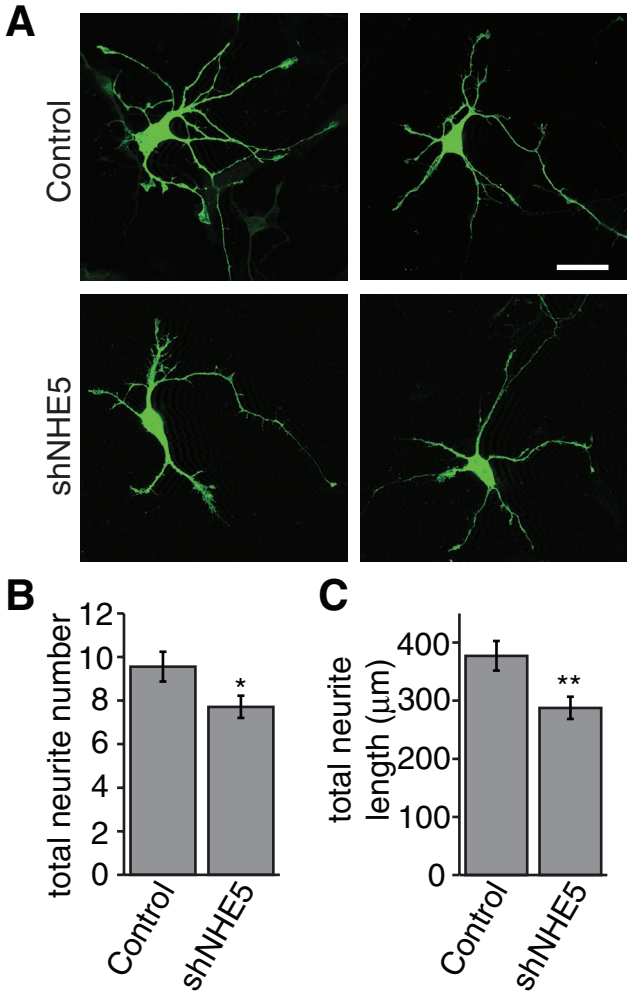

FIGURE 10: NHE5 participates in neurite growth in primary cortical neurons. (A–C) Primary rat cortical neurons (E18) were transfected with control plasmid or plasmid encoding shRNA against NHE5, both of which also express GFP. Transfected neurons were imaged by confocal microscopy at 4 d in vitro. (A) Two examples of each transfection. Scale bar, 25 µm. Total neurite number (B) and cumulative length (C) per cell. $N = 34$ control and 38 shNHE5 cells. Error bars represent SEM. *$p < 0.05$, **$p < 0.01$, by paired Student's *t* test.

NHE3 in epithelia cells (Donowitz *et al.*, 2013). Second, whereas NHE1 suppression also influences NGF-induced neurite outgrowth, the morphological features of NHE1-knockdown cells are different from those of NHE5-knockdown cells (Figure 8). NHE1 regulates cytoskeletal remodeling by cofilin and cortactin (Frantz *et al.*, 2008; Magalhaes *et al.*, 2011), actin-binding proteins that play a central role in neurite extension (Dent and Gertler, 2003; Lowery and Van Vactor, 2009; Bernstein and Bamburg, 2010), and, therefore, impaired actin cytoskeleton remodeling may contribute to the neurite phenotype of NHE1-knockdown PC12 cells. NHE5 may play a prominent role in initiating neurite formation and polarity establishment, whereas NHE1 may promote neurite extension and branching.

The precise identification of molecular mechanisms underlying extracellular/endosomal luminal pH-dependent TrkA trafficking awaits future studies. However, there are several candidates. A small GTPase, Arf6, and its GDP/GTP exchange factor, ARNO, are recruited to early endosomal membranes by direct interaction with V-ATPase subunits in a luminal acidification–dependent manner (Hurtado-Lorenzo *et al.*, 2006). We previously proposed a model in which secretory carrier membrane proteins, a group of integral membrane proteins that shuttle among multiple organelles, guide NHE5 to the Arf6-dependent recycling circuit (Diering *et al.*, 2009). Arf6 has been suggested to target endosomally activated Rac1, a key molecule that controls NGF-induced axonal growth and growth cone guidance (Reichardt, 2006), to a specialized plasma membrane domain (Palamidessi *et al.*, 2008). It is interesting to postulate that NHE5 and V-ATPase may show close association on endosomal membranes and that their functional collaboration may activates Arf6, which in turn targets signaling molecules, including Rac1, to a membrane subdomain that induces neurite formation at this location. Indeed, endocytic recycling of Met (hepatocyte growth factor receptor; Joffre *et al.*, 2011) and vascular endothelial growth factor receptors (Nakayama *et al.*, 2013) has been suggested to be crucial for efficient signaling and Arf6 to be a key molecule in this process (Parachoniak *et al.*, 2011). In addition, a recent study showed that a pH-dependent mechanism governs recycling of galectin-3 and the low-affinity neurotrophin receptor p75 at the apical membrane of polarized epithelial cells (Straube *et al.*, 2013). The pH-sensitive recycling of unique groups of proteins and lipids may play a crucial part in cell polarity establishment.

MATERIALS AND METHODS

Cell lines

PC12 cells were transfected with pRNAT-H1 vectors (GenScript, Piscataway, NJ) containing shRNA sequences targeting NHE5 or by pRNAT-U6 vectors (GenScript) containing shRNA sequences targeting NHE1 by calcium phosphate method, and stable clones showing reduced protein expression were isolated as described previously (Diering *et al.*, 2011). Stable clones were maintained in the presence of 200 µg/ml G418 or 100 µg/ml hygromycin, and low–passage number cells were used for all experiments. A snapshot Western blot was performed to verify the suppression of the protein before experiments. PC12-based cell lines were grown in DMEM containing 5% fetal bovine serum (FBS) and 10% heat-inactivated horse serum.

Antibodies and biochemical reagents

Rabbit polyclonal anti-NHE5 antibodies were raised and characterized as previously described (Diering *et al.*, 2011). The following additional primary antibodies were used: mouse monoclonal anti-NHE1, anti-EEA1, and anti-Rab11 (BD Biosciences, San Jose, CA), mouse monoclonal anti-Na^+/K^+ ATPase α-subunit (Developmental Studies Hybridoma Bank, Iowa City, IA), mouse monoclonal anti–transferrin receptor (Zymed, San Francisco, CA), rabbit polyclonal (C-14) and mouse monoclonal (B-3) anti-TrkA (Santa Cruz Biotechnology, Santa Cruz, CA), rabbit polyclonal anti-Erk1/2 (Biosource, Camarillo, CA), and rabbit polyclonal anti–phospho-Erk, anti-Akt, and anti–phospho-Akt (Cell Signaling, Danvers, MA). The following secondary antibodies were used: Alexa Fluor 488–conjugated goat anti-mouse or Alexa Fluor 568–conjugated goat anti-rabbit (Molecular Probes, Eugene, OR) and horseradish peroxidase–conjugated goat anti-rabbit and goat anti-mouse secondary antibodies (Jackson ImmunoResearch, West Grove, PA). All biochemical reagents were of analytical grade or higher and obtained from Sigma-Aldrich (St. Louis, MO) unless otherwise indicated. Monomeric red fluorescent protein (mRFP)–tagged human Rab5 cDNA (plasmid #14437) and mRFP-tagged dog Rab7 (plasmid #14436) were obtained from Addgene (Cambridge, MA), and the inserts were subcloned into the pECFP or pmCherry vector.

Immunofluorescence confocal microscopy

PC12-based cell lines were fixed for 10 min at room temperature with 4% paraformaldehyde in phosphate-buffered saline (PBS), permeabilized with 0.1% Triton X-100 in PBS for 10 min at room temperature or fixed for 10 min by prechilled methanol–acetone (80–20% [vol/vol], −20°C) with no permeabilization, blocked with PBS containing 10% normal goat serum for 30 min, and then incubated with primary antibody in PBS containing 1% goat serum overnight at 4°C. After washing, coverslips were incubated with fluorescently labeled secondary antibodies at room temperature for 1 h. After additional washes, they were then mounted onto glass slides with Prolong Gold antifade reagent (Life Technologies, Carlsbad, CA). Confocal images were obtained with the 100×/numerical aperture 1.4 UPlanApo objective of an Olympus FV1000 (Olympus, Tokyo, Japan).

Neurite growth measurement

Neurite growth was measured as described previously (Sin *et al.*, 2009). In brief, PC12-based cell lines were plated onto collagen-coated glass coverslips and grown for 72 h in DMEM containing 1% FBS, 2% horse serum, and 50 ng/ml NGF (Cedarlane Laboratories, Burlington, Canada). After 72 h of NGF treatment, tubulins and actins were visualized by immunofluorescence microscopy with anti-tubulin antibody and fluorescently labeled phalloidin, respectively. Randomly selected fields of cells were imaged by confocal or fluorescence microscopy using a 10× magnification objective, and the number and length of neurites were measured using ImageJ software (National Institutes of Health, Bethesda, MD). All cells in a field were counted, and cells with at least one neurite extension >15 µm in length were scored as cells with neurites. For neurite length and number calculation, only cells with at least one primary neurite >15 µm in length were imaged and included in analyses. The number and cumulative length of primary neurites (extensions from the cell body of at least 10 µm in length) and secondary neurites (second- and higher-order neurites at least 5 µm in length) were measured. Data are presented as the mean total number of neurites per cell (primary and secondary neurites) or as the total length of neurites from >80 cells per condition. For rescue experiments, NHE5-knockdown cell lines were transfected with HA-tagged human NHE5, and clones stably expressing human NHE5 were used.

NGF signaling

Subconfluent PC12-based cell lines were serum starved overnight, treated with NGF (50 ng/ml) in serum-free media for the times indicated, and then lysed using 1% NP-40 in PBS containing protease inhibitor cocktail (Roche Applied Science, Indianapolis, IN). Equal amounts of protein for each condition were resolved by SDS–PAGE, and total or phosphorylated amounts of specific proteins were assessed by Western blot.

Cell-surface biotinylation

Subconfluent PC12-based cell lines were serum starved overnight and then treated with 50 ng/ml NGF or 250 nM bafilomycin A1 (LC Laboratories, Woburn, MA) in serum-free media for the times indicated. Cell-surface biotinylation was carried out as described previously (Lin *et al.*, 2007). In brief, cells were incubated with the membrane-impermeable, protein-reactive biotinylation reagent *N*-hydroxysulfosuccinimidyl-SS-biotin (0.5 mg/ml; Thermo Scientific, Waltham, MA) in PBS containing 0.1 mM $CaCl_2$ and 1 mM $MgCl_2$ (PBSCM) for 30 min at 4°C, and unreacted biotinylation reagent was quenched with 20 mM glycine in PBSCM, two times for 7 min each. Cells were then lysed in 1% NP-40 in PBS containing protease inhibitor cocktail. Equal amounts of protein were incubated overnight at 4°C with NeutrAvidin-conjugated agarose beads (Thermo Scientific). After washing of the beads with ice-cold lysis buffer, biotinylated proteins were eluted using SDS sample buffer containing 100 mM dithiothreitol, and surface-labeled proteins were resolved by SDS–PAGE and detected by Western blot. Five percent of the total lysate not subjected to NeutrAvidin beads was also resolved as a loading control.

Endosomal pH measurement

Cells were grown on collagen-coated glass-bottom dishes, serum starved for 4 h, and then incubated in Na^+-saline (130 mM NaCl, 5 mM KCl, 1 mM $MgCl_2$, 2 mM $CaCl_2$, 5 mM glucose, 20 mM 4-(2-hydroxyethyl)-1-piperazineethanesulfonic acid [HEPES]–NaOH, pH 7.4) containing 75 µg/ml fluorescein-conjugated transferrin (Molecular Probes) and 25 µg/ml Alexa Fluor 568–conjugated transferrin (Molecular Probes) for 1 h at 37°C. Cells were then rinsed three times with Na^+-saline and then imaged by confocal microscopy for up to 10 min in a temperature-controlled chamber at 37°C. Fluorescein was imaged by excitation with a 488-nm laser, and Alexa Fluor 568 was imaged using a 546-nm laser. Fluorescein is pH sensitive, whereas Alexa Fluor 568 is pH insensitive, and thus by imaging the two fluorophores together, we were able to perform ratiometric measurements of endosomal pH (D'Souza *et al.*, 1998; Gagescu *et al.*, 2000; Brett *et al.*, 2005; Ohgaki *et al.*, 2010; Diering *et al.*, 2011). To convert the fluorescein/Alexa Fluor 568 fluorescence ratios to pH, we imaged fluorescein- or Alexa-conjugated transferrin-loaded cells under pH-clamp conditions (high K^+, 10 µM nigericin, pH 6.0–7.0). In some experiments transferrin-loaded cells were imaged after treatment with the V-ATPase inhibitor bafilomycin (250–500 nM) to cause endosomal alkalinization. For early endosomal pH measurement experiments, cells were treated with the mixture of fluorescein- and Alexa Fluor 568–conjugated Tfn at 4°C for 30 min, rinsed with prechilled serum-free media, and subjected to chase incubation at 22°C for up to 15 min. Confocal images were obtained with the 100×/numerical aperture 1.4 UPlanApo objective of an Olympus FV1000 or a III-Zeiss spinning disk confocal microscope.

NHE activity assay

NHE activity was measured as described previously (Diering *et al.*, 2009). In brief, PC12 cells were loaded with 2 µM BCECF acetoxymethyl ester in HEPES-buffered saline (HBS; 130 mM NaCl, 5 mM KCl, 1 mM $MgCl_2$, 2 mM $CaCl_2$, 5 mM glucose, 20 mM HEPES-NaOH, pH 7.4) for 10 min at room temperature. Coverslips with cells attached were then mounted in a temperature-controlled recording chamber filled with HBS, placed on the microscope stage, and superfused at 2 ml/min with HBS at 34°C throughout an experiment. The dual–excitation ratio method was used to estimate pH_i using a fluorescence ratio imaging system (Atto Biosciences, Rockville, MD), and the high–$[K^+]$/nigericin technique was used to convert background-corrected BCECF emission intensity ratios into pH_i values. Intracellular acid loads were imposed by exposing the cells for 2 min to NH_4^+–choline chloride solution, followed by washout with choline chloride solution. Na^+/H^+ exchange was activated by a return to HBS in the absence or presence of the NHE1-specific antagonist cariporide (10 µM).

Neuronal cell culture and neurite growth measurement

Cortex from E18 rat was prepared as previously described (Xie *et al.*, 2001). Dissociated neurons were transfected with control or NHE5 shRNA plasmid (contains a green fluorescent protein [GFP]

expression cassette) by nucleoporation using a rat neuron nucleoporation kit (Lonza, Cologne, Germany) before plating. Electroporated neurons were plated at a density of 250 cells/mm^2 on poly-L-lysine–coated coverslips. Neurons were grown for 4 d in vitro in a humidified incubator under 5% CO_2 in neurobasal medium supplemented with 5% horse serum, 1% penicillin/streptomycin, 1% GlutaMAX, and 2% B27 supplement (Life Technologies). Neurons were fixed in 4% paraformaldehyde in PBS for 10 min and mounted on glass slides, and GFP-positive cells were imaged by confocal fluorescence microscopy. Neurite number and length were measured as previously described (Sin *et al.*, 2009) using ImageJ software.

ACKNOWLEDGMENTS

We thank Richard Huganir (Johns Hopkins University, Baltimore, MD) for help with the experiments on neurons in primary culture. This work was supported by a National Science and Engineering Research Council Discovery Grant to M.N. G.H.D. was a recipient of National Science and Engineering Research Council PGS and CGS Awards and Michael Smith Foundation for Health Research Doctoral Awards. G.H.D. is a recipient of a Canadian Institute of Health Research Postdoctoral Fellowship. Cariporide was generously provided by Sanofi (Paris, France). The Na, K-ATPase antibody developed by Douglas M. Fambrough was obtained from the Developmental Studies Hybridoma Bank developed under the auspices of the National Institute of Child Health and Human Development and maintained by the Department of Biology, University of Iowa, Iowa City, IA.

REFERENCES

Arimura N *et al.* (2009). Anterograde transport of TrkB in axons is mediated by direct interaction with Slp1 and Rab27. Dev Cell 16, 675–686.

Arimura N, Kaibuchi K (2007). Neuronal polarity: from extracellular signals to intracellular mechanisms. Nat Rev Neurosci 8, 194–205.

Ascano M, Richmond A, Borden P, Kuruvilla R (2009). Axonal targeting of Trk receptors via transcytosis regulates sensitivity to neurotrophin responses. J Neurosci 29, 11674–11685.

Attaphitaya S, Park K, Melvin JE (1999). Molecular cloning and functional expression of a rat Na^+/H^+ exchanger (NHE5) highly expressed in brain. J Biol Chem 274, 4383–4388.

Baass PC, Di Guglielmo GM, Authier F, Posner BI, Bergeron JJ (1995). Compartmentalized signal transduction by receptor tyrosine kinases. Trends Cell Biol 5, 465–470.

Bacac M, Fusco C, Planche A, Santodomingo J, Demaurex N, Leemann-Zakaryan R, Provero P, Stamenkovic I (2011). Securin and separase modulate membrane traffic by affecting endosomal acidification. Traffic 12, 615–626.

Baird NR, Orlowski J, Szabo EZ, Zaun HC, Schultheis PJ, Menon AG, Shull GE (1999). Molecular cloning, genomic organization, functional expression of Na^+/H^+ exchanger isoform 5 (NHE5) from human brain. J Biol Chem 274, 4377–4382.

Barbacid M (1994). The Trk family of neurotrophin receptors. J Neurobiol 25, 1386–1403.

Bernstein BW, Bamburg JR (2010). ADF/cofilin: a functional node in cell biology. Trends Cell Biol 20, 187–195.

Bradke F, Dotti CG (1998). Membrane traffic in polarized neurons. Biochim Biophys Acta 1404, 245–258.

Bray GE, Ying Z, Baillie LD, Zhai R, Mulligan SJ, Verge VMK (2013). Extracellular pH and neuronal depolarization serve as dynamic switches to rapidly mobilize TrkA to the membrane of adult sensory neurons. J Neurosci 33, 8202–8215.

Brett CL, Tukaye DN, Mukherjee S, Rao R (2005). The yeast endosomal $(Na^+, K^+)/H^+$ exchanger Nhx1 regulates cellular pH to control vesicle trafficking. Mol Biol Cell 16, 1396–1405.

Casey JR, Grinstein S, Orlowski J (2010). Sensors and regulators of intracellular pH. Nat Rev Mol Cell Biol 11, 50–61.

Chao MV (2003). Neurotrophins and their receptors: a convergence point for many signalling pathways. Nat Rev Neurosci 4, 299–309.

Chen ZY, Ieraci A, Tanowitz M, Lee FS (2005). A novel endocytic recycling signal distinguishes biological responses of Trk neurotrophin receptors. Mol Biol Cell 16, 5761–5772.

Clague MJ, Urbe S, Aniento F, Gruenberg J (1994). Vacuolar ATPase activity is required for endosomal carrier vesicle formation. J Biol Chem 269, 21–24.

Counts SE, Nadeem M, Wuu J, Ginsberg SD, Saragovi HU, Mufson EJ (2004). Reduction of cortical TrkA but not p75NTR protein in early-stage Alzheimer's disease. Ann Neurol 56, 520–531.

Cox GA, Lutz CM, Yang CL, Biemesderfer D, Bronson RT, Fu A, Aronson PS, Noebels JL, Frankel WN (1997). Sodium/hydrogen exchanger gene defect in slow-wave epilepsy mutant mice. Cell 91, 139–148.

Dent EW, Gertler FB (2003). Cytoskeletal dynamics and transport in growth cone motility and axon guidance. Neuron 40, 209–227.

Diab HI, Kane PM (2013). Loss of vacuolar H^+-ATPase (V-ATPase) activity in yeast generates an iron deprivation signal that is moderated by induction of the peroxiredoxin TSA2. J Biol Chem 288, 11366–11377.

Diering GH, Church J, Numata M (2009). Secretory carrier membrane protein 2 regulates cell-surface targeting of brain-enriched Na^+/H^+ exchanger NHE5. J Biol Chem 284, 13892–13903.

Diering GH, Mills F, Bamji SX, Numata M (2011). Regulation of dendritic spine growth through activity-dependent recruitment of the brain-enriched Na^+/H^+ exchanger NHE5. Mol Biol Cell 22, 2246–2257.

Dobrowolski R, Vick P, Ploper D, Gumper I, Snitkin H, Sabatini DD, De Robertis EM (2012). Presenilin deficiency or lysosomal inhibition enhances Wnt signaling through relocalization of GSK3 to the late-endosomal compartment. Cell Rep 2, 1316–1328.

Donowitz M, Ming Tse C, Fuster D (2013). SLC9/NHE gene family, a plasma membrane and organellar family of Na^+/H^+ exchangers. Mol Aspects Med 34, 236–251.

D'Souza S, Garcia-Cabado A, Yu F, Teter K, Lukacs G, Skorecki K, Moore HP, Orlowski J, Grinstein S (1998). The epithelial sodium-hydrogen antiporter Na^+/H^+ exchanger 3 accumulates and is functional in recycling endosomes. J Biol Chem 273, 2035–2043.

Flinn RJ, Yan Y, Goswami S, Parker PJ, Backer JM (2010). The late endosome is essential for mTORC1 signaling. Mol Biol Cell 21, 833–841.

Forgac M (2007). Vacuolar ATPases: rotary proton pumps in physiology and pathophysiology. Nat Rev Mol Cell Biol 8, 917–929.

Frantz C, Barreiro G, Dominguez L, Chen X, Eddy R, Condeelis J, Kelly MJ, Jacobson MP, Barber DL (2008). Cofilin is a pH sensor for actin free barbed end formation: role of phosphoinositide binding. J Cell Biol 183, 865–879.

Fujioka Y, Tsuda M, Hattori T, Sasaki J, Sasaki T, Miyazaki T, Ohba Y (2011). The Ras-PI3K signaling pathway is involved in clathrin-independent endocytosis and the internalization of influenza viruses. PLoS One 6, e16324.

Gagescu R, Demaurex N, Parton RG, Hunziker W, Huber LA, Gruenberg J (2000). The recycling endosome of Madin-Darby canine kidney cells is a mildly acidic compartment rich in raft components. Mol Biol Cell 11, 2775–2791.

Garcia-Regalado A, Guzman-Hernandez ML, Ramirez-Rangel I, Robles-Molina E, Balla T, Vazquez-Prado J, Reyes-Cruz G (2008). G protein-coupled receptor-promoted trafficking of Gbeta1gamma2 leads to AKT activation at endosomes via a mechanism mediated by Gbeta1gamma2-Rab11a interaction. Mol Biol Cell 19, 4188–4200.

Golachowska MR, Hoekstra D, van IJzendoorn IS (2010). Recycling endosomes in apical plasma membrane domain formation and epithelial cell polarity. Trends Cell Biol 20, 618–626.

Grant BD, Donaldson JG (2009). Pathways and mechanisms of endocytic recycling. Nat Rev Mol Cell Biol 10, 597–608.

Greene LA, Tischler AS (1976). Establishment of a noradrenergic clonal line of rat adrenal pheochromocytoma cells which respond to nerve growth factor. Proc Natl Acad Sci USA 73, 2424–2428.

Grimes ML, Zhou J, Beattie EC, Yuen EC, Hall DE, Valletta JS, Topp KS, LaVail JH, Bunnett NW, Mobley WC (1996). Endocytosis of activated TrkA: evidence that nerve growth factor induces formation of signaling endosomes. J Neurosci 16, 7950–7964.

Habauzit D, Flouriot G, Pakdel F, Saligaut C (2011). Effects of estrogens and endocrine-disrupting chemicals on cell differentiation-survival-proliferation in brain: contributions of neuronal cell lines. J Toxicol Environ Health B Crit Rev 14, 300–327.

Harrill JA, Mundy WR (2011). Quantitative assessment of neurite outgrowth in PC12 cells. Methods Mol Biol 758, 331–348.

Harrington AW, St Hillaire C, Zweifel LS, Glebova NO, Philippidou P, Halegoua S, Ginty DD (2011). Recruitment of actin modifiers to TrkA endosomes governs retrograde NGF signaling and survival. Cell 146, 421–434.

Hsu VW, Prekeris R (2010). Transport at the recycling endosome. Curr Opin Cell Biol 22, 528–534.
Huang EJ, Reichardt LF (2001). Neurotrophins: roles in neuronal development and function. Annu Rev Neurosci 24, 677–736.
Huotari J, Helenius A (2011). Endosome maturation. EMBO J 30, 3481–3500.
Hurtado-Lorenzo A *et al.* (2006). V-ATPase interacts with ARNO and Arf6 in early endosomes and regulates the protein degradative pathway. Nat Cell Biol 8, 124–136.
Jewell JL, Russell RC, Guan KL (2013). Amino acid signalling upstream of mTOR. Nat Rev Mol Cell Biol 14, 133–139.
Joffre C, Barrow R, Menard L, Calleja V, Hart IR, Kermorgant S (2011). A direct role for Met endocytosis in tumorigenesis. Nat Cell Biol 13, 827–837.
Jullien J, Guili V, Reichardt LF, Rudkin BB (2002). Molecular kinetics of nerve growth factor receptor trafficking and activation. J Biol Chem 277, 38700–38708.
Kozik P, Hodson NA, Sahlender DA, Simecek N, Soromani C, Wu J, Collinson LM, Robinson MS (2013). A human genome-wide screen for regulators of clathrin-coated vesicle formation reveals an unexpected role for the V-ATPase. Nat Cell Biol 15, 50–60.
Kuruvilla R, Zweifel LS, Glebova NO, Lonze BE, Valdez G, Ye H, Ginty DD (2004). A neurotrophin signaling cascade coordinates sympathetic neuron development through differential control of TrkA trafficking and retrograde signaling. Cell 118, 243–255.
Ledesma MD, Dotti CG (2003). Membrane and cytoskeleton dynamics during axonal elongation and stabilization. Int Rev Cytol 227, 183–219.
Li X, Difiglia M (2012). The recycling endosome and its role in neurological disorders. Prog Neurobiol 97, 127–141.
Lin DC, Quevedo C, Brewer NE, Bell A, Testa JR, Grimes ML, Miller FD, Kaplan DR (2006). APPL1 associates with TrkA and GIPC1 and is required for nerve growth factor-mediated signal transduction. Mol Cell Biol 26, 8928–8941.
Lin PJ, Williams WP, Kobiljski J, Numata M (2007). Caveolins bind to (Na^+, K^+)/H^+ exchanger NHE7 by a novel binding module. Cell Signal 19, 978–988.
Liu Y, Zaun HC, Orlowski J, Ackerman SL (2013). CHP1-mediated NHE1 biosynthetic maturation is required for Purkinje cell axon homeostasis. J Neurosci 33, 12656–12669.
Lowery LA, Van Vactor D (2009). The trip of the tip: understanding the growth cone machinery. Nat Rev Mol Cell Biol 10, 332–343.
Lukashova V, Jinadasa T, Ilie A, Verbich D, Cooper E, Orlowski J (2013). The Na^+/H^+ exchanger NHE5 is sorted to discrete intracellular vesicles in the central and peripheral nervous systems. In: Sodium Calcium Exchange: A Growing Spectrum of Pathophysiological Implications, ed. L Annunziato, New York: Springer, 397–410.
Magalhaes MA, Larson DR, Mader CC, Bravo-Cordero JJ, Gil-Henn H, Oser M, Chen X, Koleske AJ, Condeelis J (2011). Cortactin phosphorylation regulates cell invasion through a pH-dependent pathway. J Cell Biol 195, 903–920.
Marshansky V, Futai M (2008). The V-type H^+-ATPase in vesicular trafficking: targeting, regulation and function. Curr Opin Cell Biol 20, 415–426.
Martin TF, Grishanin RN (2003). PC12 cells as a model for studies of regulated secretion in neuronal and endocrine cells. Methods Cell Biol 71, 267–286.
Masereel B, Pochet L, Laeckmann D (2003). An overview of inhibitors of Na^+/H^+ exchanger. Eur J Med Chem 38, 547–554.
Maxfield FR, McGraw TE (2004). Endocytic recycling. Nat Rev Mol Cell Biol 5, 121–132.
Meldolesi J (2011). Neurite outgrowth: this process, first discovered by Santiago Ramon y Cajal, is sustained by the exocytosis of two distinct types of vesicles. Brain Res Rev 66, 246–255.
Mellman I, Fuchs R, Helenius A (1986). Acidification of the endocytic and exocytic pathways. Annu Rev Biochem 55, 663–700.
Miaczynska M, Pelkmans L, Zerial M (2004). Not just a sink: endosomes in control of signal transduction. Curr Opin Cell Biol 16, 400–406.
Murphy JE, Padilla BE, Hasdemir B, Cottrell GS, Bunnett NW (2009). Endosomes: a legitimate platform for the signaling train. Proc Natl Acad Sci USA 106, 17615–17622.
Nakayama M *et al.* (2013). Spatial regulation of VEGF receptor endocytosis in angiogenesis. Nat Cell Biol 15, 249–260.
Nazarewicz RR, Salazar G, Patrushev N, San Martin A, Hilenski L, Xiong S, Alexander RW (2011). Early endosomal antigen 1 (EEA1) is an obligate scaffold for angiotensin II-induced, PKC-alpha-dependent Akt activation in endosomes. J Biol Chem 286, 2886–2895.
Ohgaki R, Matsushita M, Kanazawa H, Ogihara S, Hoekstra D, van Ijzendoorn SC (2010). The Na^+/H^+ exchanger NHE6 in the endosomal recycling system is involved in the development of apical bile canalicular surface domains in HepG2 cells. Mol Biol Cell 21, 1293–1304.
Palamidessi A, Frittoli E, Garre M, Faretta M, Mione M, Testa I, Diaspro A, Lanzetti L, Scita G, Di Fiore PP (2008). Endocytic trafficking of Rac is required for the spatial restriction of signaling in cell migration. Cell 134, 135–147.
Parachoniak CA, Luo Y, Abella JV, Keen JH, Park M (2011). GGA3 functions as a switch to promote Met receptor recycling, essential for sustained ERK and cell migration. Dev Cell 20, 751–763.
Platta HW, Stenmark H (2011). Endocytosis and signaling. Curr Opin Cell Biol 23, 393–403.
Presley JF, Mayor S, McGraw TE, Dunn KW, Maxfield FR (1997). Bafilomycin A1 treatment retards transferrin receptor recycling more than bulk membrane recycling. J Biol Chem 272, 13929–13936.
Puthenveedu MA, Lauffer B, Temkin P, Vistein R, Carlton P, Thorn K, Taunton J, Weiner OD, Parton RG, von Zastrow M (2010). Sequence-dependent sorting of recycling proteins by actin-stabilized endosomal microdomains. Cell 143, 761–773.
Reichardt LF (2006). Neurotrophin-regulated signalling pathways. Philos Trans R Soc B Biol Sci 361, 1545–1564.
Sadowski L, Pilecka I, Miaczynska M (2009). Signaling from endosomes: location makes a difference. Exp Cell Res 315, 1601–1609.
Sancak Y, Bar-Peled L, Zoncu R, Markhard AL, Nada S, Sabatini DM (2010). Ragulator-Rag complex targets mTORC1 to the lysosomal surface and is necessary for its activation by amino acids. Cell 141, 290–303.
Sann S, Wang Z, Brown H, Jin Y (2009). Roles of endosomal trafficking in neurite outgrowth and guidance. Trends Cell Biol 19, 317–324.
Schenck A, Goto-Silva L, Collinet C, Rhinn M, Giner A, Habermann B, Brand M, Zerial M (2008). The endosomal protein Appl1 mediates Akt substrate specificity and cell survival in vertebrate development. Cell 133, 486–497.
Scita G, Di Fiore PP (2010). The endocytic matrix. Nature 463, 464–473.
Scott CC, Gruenberg J (2011). Ion flux and the function of endosomes and lysosomes: pH is just the start: the flux of ions across endosomal membranes influences endosome function not only through regulation of the luminal pH. Bioessays 33, 103–110.
Sigismund S, Argenzio E, Tosoni D, Cavallaro E, Polo S, Di Fiore PP (2008). Clathrin-mediated internalization is essential for sustained EGFR signaling but dispensable for degradation. Dev Cell 15, 209–219.
Sin WC, Moniz DM, Ozog MA, Tyler JE, Numata M, Church J (2009). Regulation of early neurite morphogenesis by the Na^+/H^+ exchanger NHE1. J Neurosci 29, 8946–8959.
Slessareva JE, Routt SM, Temple B, Bankaitis VA, Dohlman HG (2006). Activation of the phosphatidylinositol 3-kinase Vps34 by a G protein α subunit at the endosome. Cell 126, 191–203.
Sonawane ND, Thiagarajah JR, Verkman AS (2002). Chloride concentration in endosomes measured using a ratioable fluorescent Cl^- indicator: evidence for chloride accumulation during acidification. J Biol Chem 277, 5506–5513.
Sorkin A, von Zastrow M (2009). Endocytosis and signalling: intertwining molecular networks. Nat Rev Mol Cell Biol 10, 609–622.
Steinberg F, Heesom KJ, Bass MD, Cullen PJ (2012). SNX17 protects integrins from degradation by sorting between lysosomal and recycling pathways. J Cell Biol 197, 219–230.
Straube T, von Mach T, Hönig E, Greb C, Schneider D, Jacob R (2013). pH-dependent recycling of galectin-3 at the apical membrane of epithelial cells. Traffic 14, 1014–1027.
Straud S, Zubovych I, De Brabander JK, Roth MG (2010). Inhibition of iron uptake is responsible for differential sensitivity to V-ATPase inhibitors in several cancer cell lines. PLoS One 5, e11629.
Szabo EZ, Numata M, Lukashova V, Iannuzzi P, Orlowski J (2005). beta-Arrestins bind and decrease cell-surface abundance of the Na^+/H^+ exchanger NHE5 isoform. Proc Natl Acad Sci USA 102, 2790–2795.
Szabo EZ, Numata M, Shull GE, Orlowski J (2000). Kinetic and pharmacological properties of human brain Na^+/H^+ exchanger isoform 5 stably expressed in Chinese hamster ovary cells. J Biol Chem 275, 6302–6307.
Szaszi K, Paulsen A, Szabo EZ, Numata M, Grinstein S, Orlowski J (2002). Clathrin-mediated endocytosis and recycling of the neuron-specific Na^+/H^+ exchanger NHE5 isoform. Regulation by phosphatidylinositol 3′-kinase and the actin cytoskeleton. J Biol Chem 277, 42623–42632.
Taelman VF, Dobrowolski R, Plouhinec JL, Fuentealba LC, Vorwald PP, Gumper I, Sabatini DD, De Robertis EM (2010). Wnt signaling requires

sequestration of glycogen synthase kinase 3 inside multivesicular endosomes. Cell 143, 1136–1148.
Tsutsumi K, Fujioka Y, Tsuda M, Kawaguchi H, Ohba Y (2009). Visualization of Ras-PI3K interaction in the endosome using BiFC. Cell Signal 21, 1672–1679.
Urbanska A, Sadowski L, Kalaidzidis Y, Miaczynska M (2011). Biochemical characterization of APPL endosomes: the role of annexin A2 in APPL membrane recruitment. Traffic 12, 1227–1241.
Vaegter CB *et al*. (2011). Sortilin associates with Trk receptors to enhance anterograde transport and neurotrophin signaling. Nat Neurosci 14, 54–61.
Vanhaesebroeck B, Guillermet-Guibert J, Graupera M, Bilanges B (2010). The emerging mechanisms of isoform-specific PI3K signalling. Nat Rev Mol Cell Biol 11, 329–341.
van Weert AW, Dunn KW, Gueze HJ, Maxfield FR, Stoorvogel W (1995). Transport from late endosomes to lysosomes, but not sorting of integral membrane proteins in endosomes, depends on the vacuolar proton pump. J Cell Biol 130, 821–834.
Varsano T, Dong MQ, Niesman I, Gacula H, Lou X, Ma T, Testa JR, Yates JR 3rd, Farquhar MG (2006). GIPC is recruited by APPL to peripheral TrkA endosomes and regulates TrkA trafficking and signaling. Mol Cell Biol 26, 8942–8952.
Vaudry D, Stork PJ, Lazarovici P, Eiden LE (2002). Signaling pathways for PC12 cell differentiation: making the right connections. Science 296, 1648–1649.
Walz HA, Shi X, Chouinard M, Bue CA, Navaroli DM, Hayakawa A, Zhou QL, Nadler J, Leonard DM, Corvera S (2010). Isoform-specific regulation of Akt signaling by the endosomal protein WDFY2. J Biol Chem 285, 14101–14108.
Wang E, Brown PS, Aroeti B, Chapin SJ, Mostov KE, Dunn KW (2000). Apical and basolateral endocytic pathways of MDCK cells meet in acidic common endosomes distinct from a nearly-neutral apical recycling endosome. Traffic 1, 480–493.
Weisz OA, Rodriguez-Boulan E (2009). Apical trafficking in epithelial cells: signals, clusters and motors. J Cell Sci 122, 4253–4266.
Winckler B, Mellman I (2010). Trafficking guidance receptors. Cold Spring Harb Perspect Biol 2, a001826.
Xie C, Lovell MA, Xiong S, Kindy MS, Guo J, Xie J, Amaranth V, Montine TJ, Markesbery WR (2001). Expression of glutathione-*S*-transferase isozyme in the SY5Y neuroblastoma cell line increases resistance to oxidative stress. Free Radic Biol Med 31, 73–81.
Zoncu R, Bar-Peled L, Efeyan A, Wang S, Sancak Y, Sabatini DM (2011). mTORC1 senses lysosomal amino acids through an inside-out mechanism that requires the vacuolar H^+-ATPase. Science 334, 678–683.

Supplemental Materials

Molecular Biology of the Cell

Diering et al.

Supplementary Figure 1

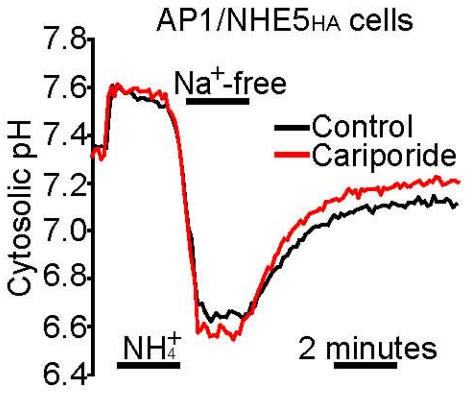

Supplementary Figure 1 NHE5 is resistant to cariporide. NHE-deficient AP-1 cells stably expressing human HA-tagged NHE5 (AP-1/NHE5HA) were loaded with the pH-sensitive dye BCECF. Cells were then subjected to a cytosolic acid load by briefly exposing cells to NH_4Cl solution followed by washout with Na^+-free solution. NHE activity was induced by reintroducing NaCl-solution with or without the NHE1-specific inhibitor cariporide. Recovery from the cytosolic acid load was observed in the absence or presence of cariporide suggesting that NHE5 is resistant to cariporide. Traces represent the mean of cytosolic pH measurements obtained simultaneously from 53 control or 70 cariporide-treated cells and are representative of three independent experiments.

Supplementary Figure 2

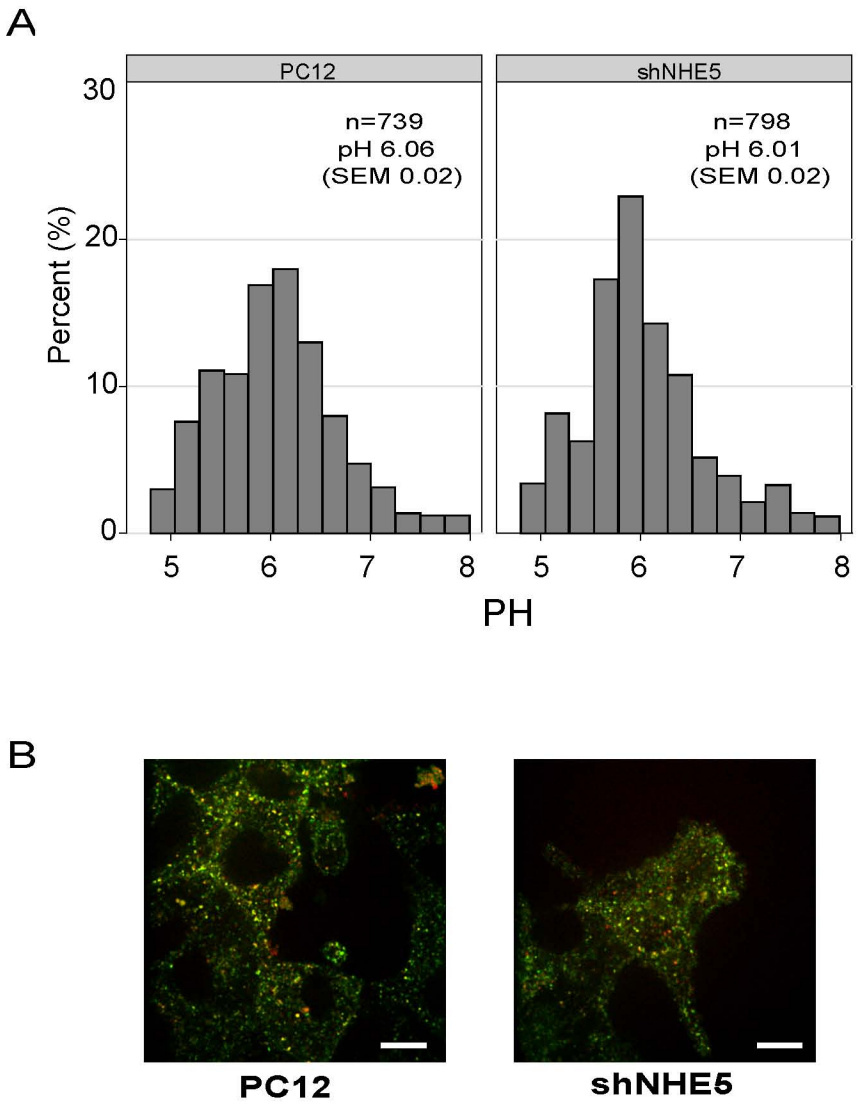

Supplementary Figure 2: Early endosome pH is not affected by shNHE5 in PC12 cells.
(A) PC12 and shNHE5 cells were treated with the mixture of fluorescein- and Alexa 568-conjugated Tfn at 4°C for 30 minutes. After quick rinse, the cells were quickly transferred to the microscope stage and subjected to chase-incubation at room temperature for 15 minutes. Images of early endosomes were captured and pH was determined as described in Materials and Methods.Corresponding pH was extrapolated by inverse regression, based on the data collected with known pH buffers with clamp. $p>0.05$ by Student's t test comparing the mean pH in two cell lines.
(B) Representative images for the pH measurement experiments.
Green:Tfn-fluorescene, Red: Tfn-Alexa568. Scale bar = 10 μm.

Supplementary Figure 3

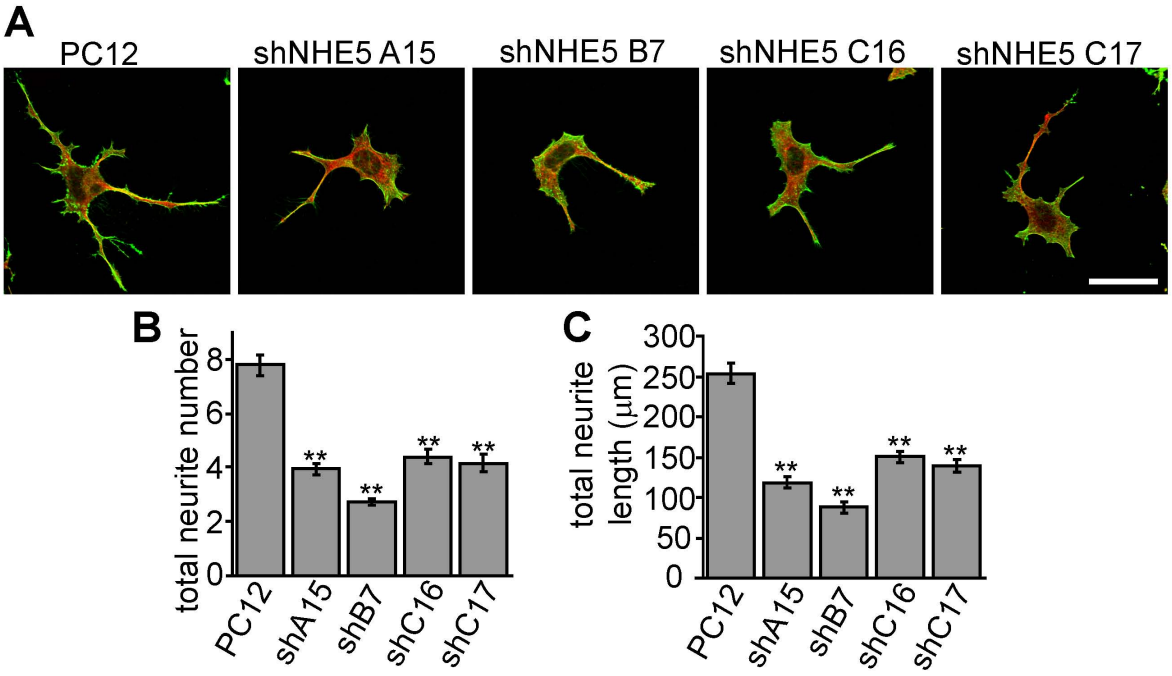

Supplementary Figure 3 Neurite growth in different PC12 cell lines stably expressing NHE5 shRNA.

(A) PC12 cells or stable clones expressing NHE5 shRNA A, B or C were treated with 50 ng/mL NGF for 72 hours to induce differentiation. Cells were labelled to visualize actin (green) and tubulin (red) in individual cells that had clearly differentiated (at least one neurite ≥ 15μm in length). N ≥80 cells per condition; error bars represent SEM; **, $p<0.01$ (Student's t-test) for difference from PC12 control cells.